Journal of Hydrology: Regional Studies 44 (2022) 101207

Contents lists available at ScienceDirect

Journal of Hydrology: Regional Studies

journal homepage: www.elsevier.com/locate/ejrh

Evaluation of climate variability on sustainability for transboundary water supply in Chihuahua, Mexico

Marusia Renteria-Villalobos [a], R.T. Hanson [b,*], Christopher Eastoe [c]

[a] Universidad Autónoma de Chihuahua, Periférico R. Almada Km 1, Chihuahua C.P. 33820, Mexico
[b] One-Water Hydrologic, LLC San Diego, CA, USA
[c] Retired, University of Arizona, Department of Geosciences, Tucson, AZ, USA

ARTICLE INFO

Keywords:
Climate variability
Climate change
Sustainability
Conjunctive water use
Water demand
International treaty deliveries
Land use
Surface-water management

ABSTRACT

Study region: This is study of the Rio Conchos Watershed, Chihuahua, Mexico.
Study focus: This study provides assessment of climate variability from analysis of instrumental climate and reservoir operations data, plus nearby tree-ring indices in Chihuahua, Mexico. Water demand include international treaty deliveries, growing agricultural land use, and intensified crop production. Analysis of climate cycles includes frequency analysis of local multidecadal instrumental hydrologic time series and multi-century tree-ring indices. In addition, tree-ring indices were compared with ^{14}C content in tree rings to assess the presence of the millennial solar cycle.
New hydrological insights for the region: Most of the climate variability within inter-annual to interdecadal periods are aligned with Pacific Decadal Oscillation (PDO)-like climate cycles. New multi-century climate cycles were discovered from tree-ring indices that have a profound impact on sustainability of food and water security. Historical droughts of 8-year average duration within PDO-like cycles that span longer (12–43 year) periods were newly identified which are longer than the 5-year delivery cycles used in the 1944 International Treaty of the Rivers. Mega-droughts were discovered to occur within multi-century climate cycles. Multi-century cycles identified in tree-ring indices were likely driven by solar luminosity changes from the millennial solar cycle and not just recent anthropogenic climate change. Climate variability and temperature increases will further amplify cycles of supply and demand and exacerbate sustainability, mitigation, and management strategies. Conjunctive use combined with reservoir operations will broaden sustainability portfolio of options, reducing demand effects as well as enhance supply options and replenishment effects.

1. Introduction

The overreaching problem is that mega-droughts and multidecadal wetter and drier periods occur within multidecadal driven by AMO and PDO cycles and within multi-century cycles influenced by changes in solar radiation from the Millennial Climate Oscillation (MCO) (ENC, 2021) that need to be considered along with Anthropogenic Climate Change (ACC) to prepare for sustainability. Alignment of management cycles with local climate cycles and related global climate drivers is fundamental to successful development

* Corresponding author.
E-mail addresses: mrenteria@uach.mx (M. Renteria-Villalobos), RandyTHanson@gmail.com (R.T. Hanson), eastoe@email.arizona.edu (C. Eastoe).

https://doi.org/10.1016/j.ejrh.2022.101207
Received 7 December 2021; Received in revised form 13 March 2022; Accepted 8 September 2022
Available online 12 October 2022

of sustainability and mitigation strategies. To steward the water resources and help achieve both sustainability and adaptability, resource management systems need to be able to assess climate change and variability linkages at different time scales that include: Operations/Uses (Seasonal to multi-year); Governance/Management (Seasonal to inter-decadal); and Capital-Improvement Projects/Infrastructure (Inter-annual to multi-century). Climate cycles that drive the supply and demand for water are largely unknown for transboundary watersheds and aquifers and remain relatively unknown along the US-Mexico border reaches of the Rio Grande River such as the Rio Conchos River watershed (Fig. 1).

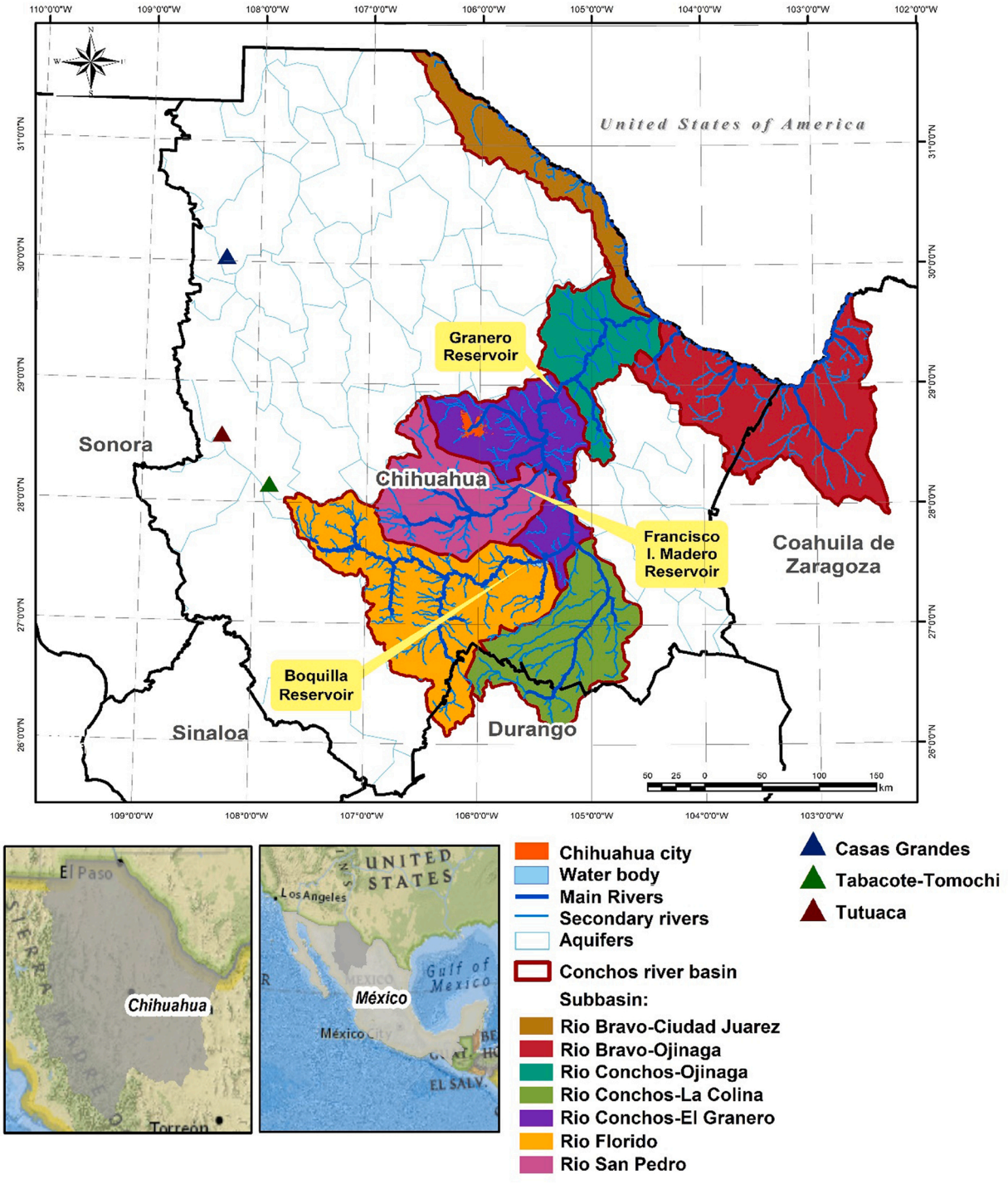

Fig. 1. Map showing the sampling points locations: three reservoirs, related watersheds, and tree-ring index sites.

Climate change, combined with growing human demand for water and evolving land use, is amplifying a crisis in demand relative to the supply of water resources, along with related issues of food and land-use security (Hanson et al., 2012; Vörösmarty et al., 2000). Climate change encompasses nonperiodic changes in global or regional climate patterns, in particular a change apparent from the mid 20th century onwards, and is attributed largely to increased levels of atmospheric carbon dioxide produced from fossil fuel use. Climate variability is driven by both oceanic and atmospheric forcings which are also potentially influenced by cycles of change in solar luminosity at millennial-scale (Clemens, 2005). This solar cycle, estimated at 1,470 years, has been the possible contributor to glacial climate cycles (Braun, 2005) and climate variability driven by millennial-scale solar variability through the Holocene (Zhao et al., 2021). Climate variability includes all the quasi-periodic climate variations lasting longer than individual weather events with periods from interannual and decadal to multiple-century duration and, consequently, is a critical factor influencing water supply and demand. Sustained dry periods spanning two or more decades are referred to as mega-droughts. These extreme climate events now identified as part of the ongoing anthropogenic climate change (Hegerl et al., 2007) also were common in the past resulting in the rise, fall, and migration of many civilizations over the past 10,000 years (Fagan, 2008).

The major periodic climate forcings juxtaposed in the study area include the Pacific/North American Oscillation (PNA, <1–4 year cycle), El Niño Southern Oscillation (ENSO, 2–7 years), the North American Monsoon System (NAMS, 7–10 years) (Hanson et al., 2006; Gutzler, 2004; Adams and Comrie, 1997), the Pacific Decadal Oscillation (PDO 11–30 years) (Mantua et al., 1997, Mantua and Hare, 2002), and the Atlantic Multidecadal Oscillation (AMO, 30–80 years) (Kuss and Gurdak 2017; Velasco et al., 2014; Gurdak et al., 2009; Deser, 2010). The Interdecadal Pacific Oscillation (IPO) (Henley et al., 2015) and North Atlantic Oscillation (NAO) may also contribute to climate variability, but are largely aligned with these other oceanic indices (Deser, 2010).

Previous continental-scale studies addressed relations of decadal-scale variability (Cayan et al., 1998) in relation to ENSO cycles (McCabe and Dettinger, 1999), related sea-surface temperature variability (Deser et al., 2010), relations of megadroughts, and monsoon variability to PDO cycles (Parsons et al., 2018; Henley et al., 2015; Newman et al., 2003, 2016; Meehl and Hu, 2006), and to AMO cycles (Hu and Feng, 2012; Nigam et al., 2011) that also may drive global-scale variability (Young-Min et al., 2020). Both Pacific and Atlantic oceans influence multidecadal drought frequency (McCabe et al., 2004) through influence on atmospheric dynamics (Erb et al., 2020). The collapse of northern hemisphere monsoons over multidecadal to multi-century scales (super droughts) may be related to North Atlantic sea-surface temperatures (AMO cycles) and northern hemisphere temperatures over the last millennium based on speleothem data (Asmerom et al., 2013). However, Eastoe and Dettman (2016) cast doubt on the interpretation of speleothem isotope data in terms of precipitation amount. The mechanisms of decadal-drought variability encompass these phenomena, an adequate understanding of which may lead to the predictability of drought beyond seasonal to interannual timescales (Seager and Ting, 2017). The Medieval Warm Period and Little Ice Age may be climate responses to longer-term natural cycles of solar radiative forcing (Mann et al., 2009). While water-resource and climate analysis methods have advanced in recent decades, there still remain many areas where the relationship between supply and demand of water resources remains unknown and not considered in the context of historical or future climate variability.

Cycles of climate variability affect the sustainability of transboundary water resources as well as related management and governance. Nevertheless no comprehensive analysis of climate variability spanning decades to centuries exists for the US-Mexico transboundary region. Additionally, climate cycles that drive the supply and demand for water are unknown for transboundary watersheds and aquifers and remain relatively unknown along the US-Mexico border reaches of the Grande River. Mega-droughts and their potential relationship to long-term climate cycles and known periodic climate drivers has not been previously analyzed in this part of transboundary northern Mexico. While Williams et al. (2020) consider the period 2000 – 2019 as a modern mega-drought the relation of this to historical mega-droughts remains uncertain. Climate variability and related supply-and-demand drivers within regional transboundary watersheds like the Rio Conchos in Chihuahua, Mexico, need to be re-assessed in the context of conjunctive use with due attention to both surface-water reservoir operations and potential use of aquifer storage as well as the long term factors that control them. While some studies have analyzed hydrologic time series and tree-ring indices for regional drought (Woodhouse et al., 2012), the combined analysis of these data was lacking and needed to answer some fundamental management and sustainability questions. What are the major drivers of climate cycles and how do they affect transboundary water resources as well as related management and governance within climate change and variability? Are the mega-droughts and multidecadal wetter and drier periods occurring within multi-century cycles influneced by solar radiation within the millenial solar cycle?.

This study estimates climate cycles over multiple time scales from new data and novel estimations of hydrologic and climate variability analysis through: a) analysis of the instrumental records assessment at three man-made surface-water reservoirs in the transboundary Rio Conchos watershed, tree-ring indices from nearby sites in Chihuahua, Mexico (Fig. 1), and global data for ^{14}C in biomass as a proxy for solar luminosity; b) a new broader approach to assessing attributes of climate variability, with implications for conjunctive-use operations of man-made reservoirs in the Rio Conchos watershed; and c) a re-evaluation of the cycles of surface-water deliveries from Mexico required under the 1944 Treaty of the Rivers (USA-Mexico, 1944). These cycles are used to estimate the range of historical drought, their potential relation to known climate indices, and their potential relationship to international treaty water-delivery obligations. In turn, this will help understand how climate variability affects transboundary water supply, related reservoir operations, and transboundary governance within the Rio Conchos watershed, and support future hydrologic model and sustainability frameworks for management and governance of water and land in this US-Mexico transboundary region of the Rio Grande River.

1.1. Previous studies

The Mexican Drought Atlas (MXDA) documents a history of droughts over the past 600 years (1400 – 2012) from tree-ring

reconstructions (Stahle et al., 2016), but does not relate this history to climate indices. Droughts affecting all of Mexico have been rare over the past 600 years and their frequency has not increased, though. selected droughts occurred (Stahle et al., 2016) (Fig. 2).

Extreme wet-year periods also have occurred, as documented in California for the Central Valley Delta from tree-ring index reconstruction (Malamud-Roam et al., 2006) and for the Rio Colorado (Woodhouse and Lukas, 2006). Since 1900, several exceptional wet periods have occurred in Western North America, including 1905–07, 1917, 1939–42, 1957, 1969, 1978, 1983–86, 1998, and 2011. Prolonged periods of drought (or wet climate) may include shorter wet (or dry) events; as shown for dry periods of 10–45 years duration in coastal Ventura, California, over the interval 1770–1995 CE (Hanson et al., 2003). Analysis of long-term aridity in the Western United States indicates that the current mega-drought is more severe than previous events estimated from the historical record (Cook et al., 2004) and the past holds insights for future climate (Alley, 2003). Environmental sustainability has been afffected by recent extreme drought, which threatens to limit the allocation of water resources in the western USA and Mexico. For example, the Rio Grande River at Elephant Butte Reservoir is at 4% of capacity (https://www.usbr.gov/newsroom/#/news-release/3958) in August, 2021, and there is a call for a shortage declaration for 2022 on Lake Meade on the Lower Colorado River (http://crc.nv.gov/index.php?p=info&s=drought) at 34% of capacity in October, 2021 (https://www.usbr.gov/lc/region/g4000/weekly.pdf). Future climate variability is expected to lead to repeated water-supply crises in the Rio Grande Basin (Mu and Ziolkowska, 2018).

The Rio Conchos is one of the largest contributors of surface water from Mexico to the Rio Grande, as well as to local irrigation and urban-water supply (Cervera Gómez, 2008). Operation of the three major reservoirs in Rio Conchos watershed is affected by the Treaty of the Rivers between the USA and Mexico (USA-Mexico, 1944; Mumme, 2019) with an earlier treaty (USA-Mexico, 1906). Contributions from six tributaries within Mexico, including the Rio Conchos, are required to provide deliveries from Mexico to the Rio Grande (Rio Bravo). Dry periods occurred on the Rio Conchos, in 1940, 1948, 1950–51, 1956–57, 1959, 1969, 1982, 1985, 1994–95, and 1997–98, and wet river-climate conditions occurred in 1938, 1941–42, 1958, 1966, 1968, 1978, 1981, 1984, 1986, and 1991 (Cervera Gómez, 2008). More recently, the reconstruction of streamflows from tree-rings for the Rio Conchos (Martínez-Sifuentes et al., 2020) estimated extreme hydroclimate events and identified several 10-year droughts over the past 243 years. Similarly, Woodhouse et al. (2012) identified regional droughts across the entire Rio Grande and Rio Conchos watersheds over the past four centuries in the 1770 s, 1890 s and 1950 s. Such extreme periods have affected local water use and treaty-delivery obligations, with the National Commission of Water (CONAGUA) recently implementing modifications to reservoir operations (Enciso, 2020). Relations between drought, land use, native riparian vegetation, and soil salinity were identified from 10 years of remote sensing images (Gutierrez et al., 2004) that highlighted additional issues of conjunctive use in the Rio Conchos Basin. This watershed is also undergoing transitions in types of agriculture and growth of other water uses (Walsh, 2009).

The 1950 s and 1990 s droughts in the Rio Conchos basin were compared and contrasted in terms of changes in the mean and variability of stream inflows, and implications for delivery obligations to the Rio Grande under the 1944 Treaty over five-year periods (Cervera Gómez, 2008). The 1944 Treaty considers “extraordinary drought” but there is no metric or threshold that delineates this condition or specifies contingent responses. Instead, the Treaty simply reassigns any deficit in delivery to the next five-year period. This assessment of droughts in the Rio Conchos basin was based on the Palmer Standardized Drought Index (PDSI) for Ojinaga, Texas from 1895–2000 (Cervera Gómez, 2008). However the PDSI is an indicator of soil moisture normalized to average conditions during the period of observation, and therfore may not identify longer droughts that might emerge from more extended periods of observation. Using a drought threshold of PDSI < -0.5, the 1950 s drought lasted seven years (86 months), and between 1992 and 1998, 7.4 years (89 months) including four years (45 months) of intense drought. These two droughts showed differences in stream inflow for the two upstream reservoirs in the Rio Conchos watershed. The most recent modification to the 1944 Treaty, Minute 325 (IBWC/CILA, 2020), provides for supplemented deliveries in light of deficits from 2015 to 2020. However, this action does not mitigate long-term

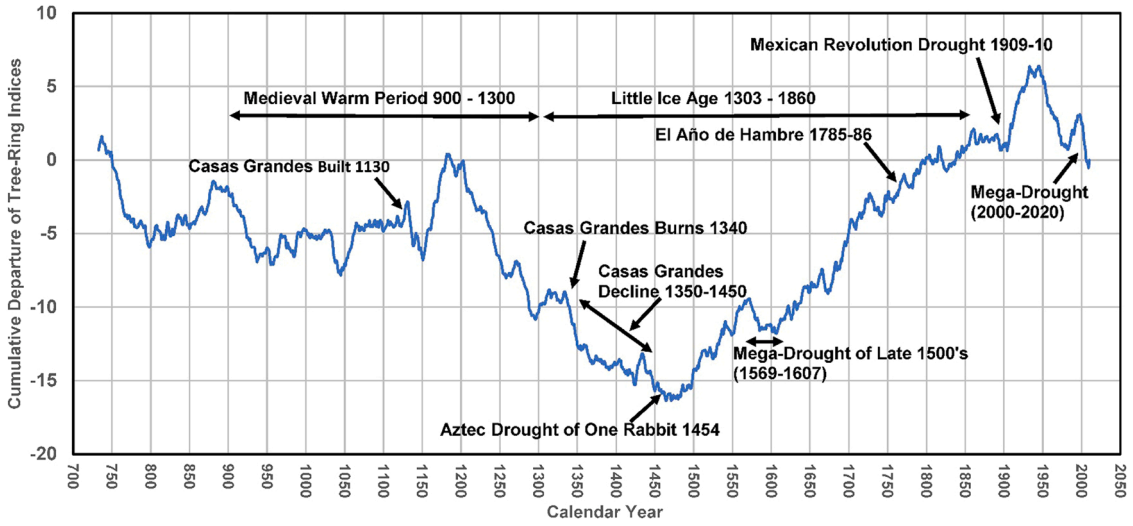

Fig. 2. Cumulative Departure curve from the Casas Grande tree-ring indices (733–2010 CE) with related climate and cultural events.

water-management issues or provide guidance for future crises arising from climate variability and prolonged droughts.

Climate forcing has been recognized through empircal analysis as a driving mechanism of change in hydrologic systems (Hanson, 2003; Dickinson et al., 2004; Hanson et al., 2004, 2006, 2009, 2020; Gurdak et al., 2009; Hanson, 2015; Velasco et al., 2017). Periodic forcings collectively contribute to wet and dry periods that control water supply-and-demand variations. At local and regional scale, wet and dry periods result from the interaction of multiple climate cycles and related climate drivers. Climate cycles operate at different frequencies and amplitudes, and their effects in southwestern North America vary as they move into and out of phase with each other (Hanson et al., 2006, 2020). Climate variability in numerous other watersheds of Southwestern North America has been studied with frequency analysis. In California, these include Central Valley (Faunt et al., 2009), Mojave River Basin, (Hanson et al., 2004), Pajaro Valley (Hanson, 2003), Santa Clara-Calleguas Basin (Hanson et al., 2003), coastal Southern California (Hanson et al., 2009), and the Santa Clara Valley (Hanson, 2015), as well as in Arizona, in Tucson Basin and San Pedro Valley (Hanson et al., 2006), and the transboundary region of the Lower Rio Grande (Hanson et al., 2020) in Texas and New Mexico, USA and Conejos-Medanos, Chihuahua, Mexico. Frequency analysis also was used to explore the principal aquifers across the USA (Kuss and Gurdak, 2014).

Multi-century cycles are evaluated with tree-ring indices and ^{14}C data. Changes in the production rate of ^{14}C in the upper atmosphere provide a proxy for changes in solar luminosity, provided lag and attenuation arising from the properties of atmospheric, biomass, and oceanic reservoirs of ^{14}C are taken into account (Beer et al., 2012). The ^{14}C content of the near-surface carbon reservoir (lower atmosphere plus biomass) is the integrated result of changes in ^{14}C production over thousands of years. Changes in production rate for cycles of 1000, 100 and 10 years appear as inflections of biomass ^{14}C content with lags of about 125, 10 and 2 years, respectively (Beer et al., 2012, Fig. 13.5.3.2–2).

2. Methodlogy

2.1. Study area

The study area, in the middle and lower areas of the Rio Conchos Watershed of southeastern Chihuahua, Mexico, of 74,372 km^2 covers 61% of the watershed (Fig. 1) including three reservoirs in this arid region, where rainfall does not exceed 400 mm/year. Rains are abundant in the summer (June-October), annual temperatures range between 18 and 20 °C, and maximum temperatures are up to 40 °C (INEGI, 2017). Of the six tributaries that flow into the lower Rio Grande from Mexico, the Rio Conchos is the largest contributor to the Treaty's Mexican delivery obligation, and its watershed makes up about half of the Rio Grande watershed in Mexico (Cervera Gómez, 2008). Three reservoirs support local uses of water for agriculture, water supply, recreation, power production, ecological flows, and flood control. Lago Toronto (La Boquilla) and Luis L. León (El Granero) reservoirs are on the Rio Conchos. The Francisco I. Madero (FIM) reservoir is located on Rio Conchos tributary, San Pedro River. La Boquilla and FIM reservoirs store water for the largest Irrigation District DR-005 in Delicias, and El Granero reservoir supplies water for the Irrigation District 090 in Bajo Río Conchos.The DR-005 covers 67,275 ha with more than 8,113 water users while the DR-090 covers 4,077 ha with 955 water users (SINA-CONAGUA, 2018). Irrigation consumes 95% of available water (SIAP, 2020). The combined utility capacity of the three reservoirs is 3,370 Mm^3 with 82% in La Boquilla, and 8% and 10% in FIM and El Granero, respectively.

Tree-ring analyses were completed just northwest of the reservoir watersheds (Cook et al., 2020; Stahle et al., 2016) (Fig. 1). Tree-ring indices from sites near Casas Grandes, about 300 km northwest of the Rio Conchos and San Pedro Watersheds, provides the longest record (733–2010 CE). Casas Grandes (Paquimé), located in an arid plain bounded on the west by the Sierra Madre Occidental, was built about 1130 C.E. in the middle of the Medieval Warm Period (900–1300 CE). It relied on irrigation for agriculture from the Casas Grandes or San Miguel Rivers. It was one of few pre-Columbian civilisations with a water well and sewer systems, indicating a long history of conjunctive use in this region. Colonial settlers also started irrigation systems as early as the 1580 s that included conjunctive use (Saldaña, 2012). Casas Grandes burned in 1340 and slowly declined from 1350 to 1450 (Fig. 2). The Tutuaca (1534–2012 CE) and Tabacote-Tomochi (1583–1993 CE) tree-ring data provide shorter records from the Sierra Madre Occidental to the southwest of Casas Grandes, in the Temosachi and Guerrero municipalities, respectively. While the analysis of climate variability with frequency methods is similar to other studies worldwide, this study also incorporates analysis of climate indices and tree-ring indices for longer time periods relevant to alignment with cycles of management and governance, as well as multi-decade infrastructure projects.

2.2. Sources and processing of data

Analysis of climate cycles for this study includes frequency analysis of local multidecadal instrumental hydrologic time series and multi-century tree-ring indices. Instrumental data include monthly precipitation, July minimum temperature and temperature differences, and reservoir attributes including storage, releases, and evaporation (CONAGUA, 2020a, Central Water and Sanitation Board JCAS, 2013). From these data, seasonal to decadal variability has been determined for 1950–2019 with seasons representing the seasons of a calendar year. Climate indices used for additional correlation analysis in this study included the AMO for 1856–2020 (NOAA_AMO, 2020), PDO for 1854–2020 (NOAA_PDO, 2020), and ENSO34 for 1871–2020 (NOAA_ENSO, 2020). While climate indices for NAMS were developed based on precipitation (Gutzler, 2004) and vapor movement (Hanson et al., 2006), no NAMS index was used for analysis in this study. Instead the range of years for NAMS periodicity is used for comparison with frequency analysis. Decadal to millennial climate variability has been determined from tree-ring indices for Casas Grandes (Cook et al., 2020; Stahle et al., 2016), Tabacote-Tomochi (Stahle et al., 2002), and Villanueva Tutuaca (Stahle et al., 2016). In addition, tree-ring indices are compared with ^{14}C content in tree rings spanning the interval 733–1953 CE (compiled by Eastoe et al., 2019).

The spectral analysis of hydrologic variability is statistically compared with reported climate-cycle intervals and time series and range of cycles of climate indices (AMO, PDO, NAMS, ENSO). to assess the similarity and provide statisitical inference between variability in hydrologic time series and known climate-cycle drivers (Hanson et al., 2004, 2006). All time series are first converted to cumulative departure curves which embeds serial correlation and provides a surrogate for the interannual climate variability rate (i.e. first derivative). Cumulative-departure time series are analogous to time series representing changes as hydrologic accumulation or depletion such as groundwater levels for changes in groundwater storage, reservoir stage for changes in reservoir storage, and the accumulation of ^{14}C in biomass. The cumulative-departure curves are detrended with a low-order polynomial because most time series encompasses fragments of even larger cycles as the method was originally described by Hanson et al. (2004). The cumulative-departure time series and the residuals from 4th-order polynomial detrending are analyzed using singular spectral analysis (SSA) to estimate the periodic frequencies that can be summed to represent the historical cumulative-departure residual time series. All frequency analysis used the established methods of the United States Geological Survey's HydroClimATe Toolkit (Dickinson et al., 2014). This toolkit facilitates climate variability analysis methods developed by Hanson et al. (2004) including the Singular Spectral Analysis methods (Dettinger et al., 1995). All frequency analyses were significant with respect to red noise. Climate change and the amplification of climate variability within climate change, can potentially result in more extreme events as well as nonstationarity of the mean and variance of climate parameters (Milly et al., 2008, 2015). However, weak-stationarity appears to persists in frequency analysis of historical and future climate cycles (Hanson et al., 2004, 2006, 2012).

The estimated cycles are compared with the typical cycles of climate indices of known climate drivers, AMO, PDO, NAMS, and ENSO. ENSO has two modes, El Niño and La Niña, that differ from other climate drivers in their patterns and teleconnections (Gurdak et al., 2009). Previous frequency analysis shows that PDO also has two modes with periods of about 10–15 years and 24–30 years. While others have studied surrogates for soil moisture using the normalized PDSI, these studies did not collectively address natural and anthropogenic variability on multiple time scales needed for water-resource management. Additionally, PDSI is not a reliable indicator for longer periods or for conjunctive use in agricultural lands where soil moisture is typically well managed through irrigation.

Data from the three reservoirs were analyzed to provide an integral depiction of their recent historical condition and sustainability under variable climate. Analysis of reservoir operations in the context of historical performance relative to climate leaves certain issues unaddressed. It includes the operation of the reservoirs in response to multiple types of demand governed by a hierarchy of operating rules that attempt to mitigate disparities between supply and demand while taking account of diverse requirements such as irrigation, recreation, power generation, and flood safety. Strategies for mitigating risk, maximizing reliability and optimizing storage as climate changes reaffirms the important role of reservoir capacitance under increased stress from climate change plus human demand (Ehsani et al., 2017) for a series of transboundary reservoirs in the northeastern United States. Reservoir operations become even more critical in arid northern Mexico and the entire USA-Mexico transboundary region. For example, drought has curtailed releases from Elephant Butte and Caballo reservoirs on the Rio Grande, resulting in major increases of groundwater use to supplement surface-water irrigation and Treaty deliveries (Hanson et al., 2020; Ferguson and Llewellyn, 2015). As both supply and demand contribute to the balance of sustainbility, recent changes in agricultural demand are also competing with treaty deliveries obligations from Mexico to the Rio Grande. Finally, the estimated hydrologic cycles are compared with known cycles from climate indices and to requirements of 5-year Treaty surface-water delivery periods from Mexico.

Tree-ring indices, as regional indicators of changing precipitation and temperature, allow climate-variability analysis over centuries across Southwestern North America (Salzer and Kipfmueller, 2005). Such analyses not only provide longer time periods (Hanson et al., 2004) but also indicators of tree and forest health subject to drought and climate variability (Anderegg et al., 2013). While the Twentieth Century Reanalysis Project (20CR) compiled global atmospheric data (Compo et al., 2011) since 1871 for improving and comparing the skill of climate models, they did not include ice core, tree-ring, or solar luminosity proxy data. Such information may provide constraints on climate change and climate variability over decadal to millennial-scale periods. It could be used to drive and constrain models and better understand the longer cycles of climate variability and now climate change too.

Speleothem data provide similar information on longer term climate variability. Asmerom et al. (2013) suggested a positive correlation between NAMS and AMO in the context of multidecadal to multi-century collapse of northern hemisphere monsoons like NAMS. The speleothem record indicates that PDO cycles modulate the NAMS across Southwestern North America, and those super droughts coincided with the Medieval Climate Anomaly (Warm Period) and the Little Ice Age (Fig. 2). This illustrates how droughts occur within longer wetter and drier cycles. These longer multi-century cycles may be related to the millennial sun cycle (called the Eddy cycle, Zhao et al., 2021) with the most recent cycle embedding the Medieval Warm period and Little Ice Age (Fig. 2).

The analysis of tree rings and ^{14}C data from tree rings was performed to identify correlations between overlapping datasets for the Casas Grandes tree rings (733 – 2010 CE) compared with 14 C content in tree rings spanning the interval 733–1953 CE (compiled by Eastoe et al., 2019), in order to examine whether solar luminosity influences the tree-ring index time series for periods on the order of 100 and 1000 years. Both datasets are filtered (using moving averages) and detrended (using fitted 3rd-order polynomials) to enhance the graphical depiction of cycles at each time scale. The ^{14}C dataset includes high-precision measurements on the cellulose fraction of dendrochronologically-dated wood by liquid scintillation counting (998–1953) at laboratories in Tucson (Eastoe et al., 2019) and Seattle, USA (Stuiver et al., 1998), and by accelerator mass spectrometry (prior to 998) in Nagoya, Japan (Miyahara et al., 2004; Miyake et al., 2012, 2013). The ^{14}C data are plotted as $-\Delta^{14}C$ (Stuiver and Polach, 1977), a parameter that accounts for mass-dependent fractionation and radioactive decay of ^{14}C. The production of ^{14}C in the upper atmosphere is a proxy for solar luminescence, provided lag and attenuation arising from the properties of atmospheric, biomass and oceanic reservoirs of ^{14}C are taken into account (Beer et al., 2012). A ^{14}C dataset from tree-rings in the western USA and Japan (Eastoe et al., 2019) overlaps most of the Casas Grandes tree-ring index data set, and incorporates data from Stuiver et al. (1998), Miyahara et al. (2004), and Miyake et al., (2012, 2013). For the purposes of this study, periods of a century-scale and shorter length were filtered out by calculating 200-year running means for

both the ^{14}C and Casas Grande cumulative departure (CGCD) time series. Century-scale events were investigated using decadal means detrended for longer-period variation with third-order polynomial expressions. The ^{14}C data are plotted as $-\Delta^{14}C$ (Stuiver and Polach, 1977), a parameter that accounts for mass-dependent fractionation and the radioactive decay of ^{14}C.

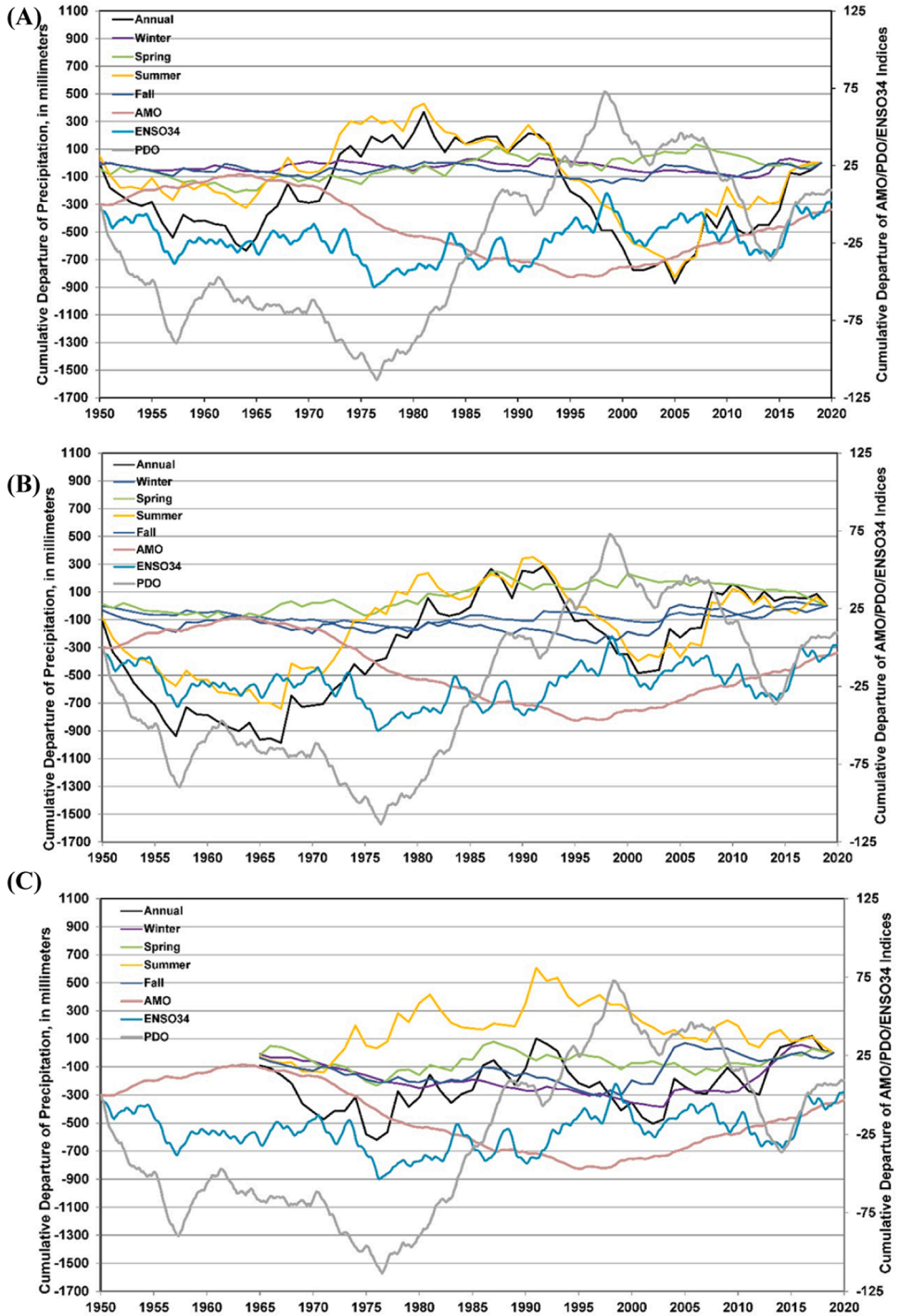

Fig. 3. Cumulative departure of annual and seasonal precipitation from (A) La Boquilla, (B) Francisco I Madero (FIM), and (C) El Granero with cumulative departure curves for AMO, PDO, and ENSO34 indices.

3. Results

3.1. Local climate cycles

Analyses of local instrumental data include precipitation and reservoir releases and storage that represent cycles of water supply, and temperature, temperature differences, and evaporation at reservoirs that represent cycles of water demand. The relatively short length of instrumental records precludes assessment of effects from the larger AMO cycles, but correlations are estimated for their period of record relative to cumulative departure time series for comparable windows of AMO, PDO, and ENSO34 indices with instrumental records.

3.1.1. Precipitation

Annual and seasonal cumulative departure of precipitation at FIM, La Boquilla, and El Granero (Fig. 3) indicate the largest variability occurs during the rainy season summer months. Summer (61 – 69%) and Spring (16 – 17%) precipitation dominating the distribution of annual precipitation. These preciptation cycles are largely coincident with PDO and ENSO/ENSO-PNA-like climate cycles (Fig. SM-1, Table SM-1). Historical winter precipitation cycles are dominated by PDO-like (48 – 83%) and ENSO/ENSO-PNA-like (10 – 35%) cycles, indicating that climate variability from PDO is more important than ENSO-like cycles. While PDO-like cycles still contribute between 49% and 78% of the variance in spring, summer, and fall these seasons also include 10–31% variability from cycles coincident with ENSO and ENSO-PNA. There is also a contribution from cycles coincident with NAMS for summer (10%) and fall (30%) at La Boquilla (fig. SM-1). Aggregate series from cumulative departures of precipitation and climate patterns show negative

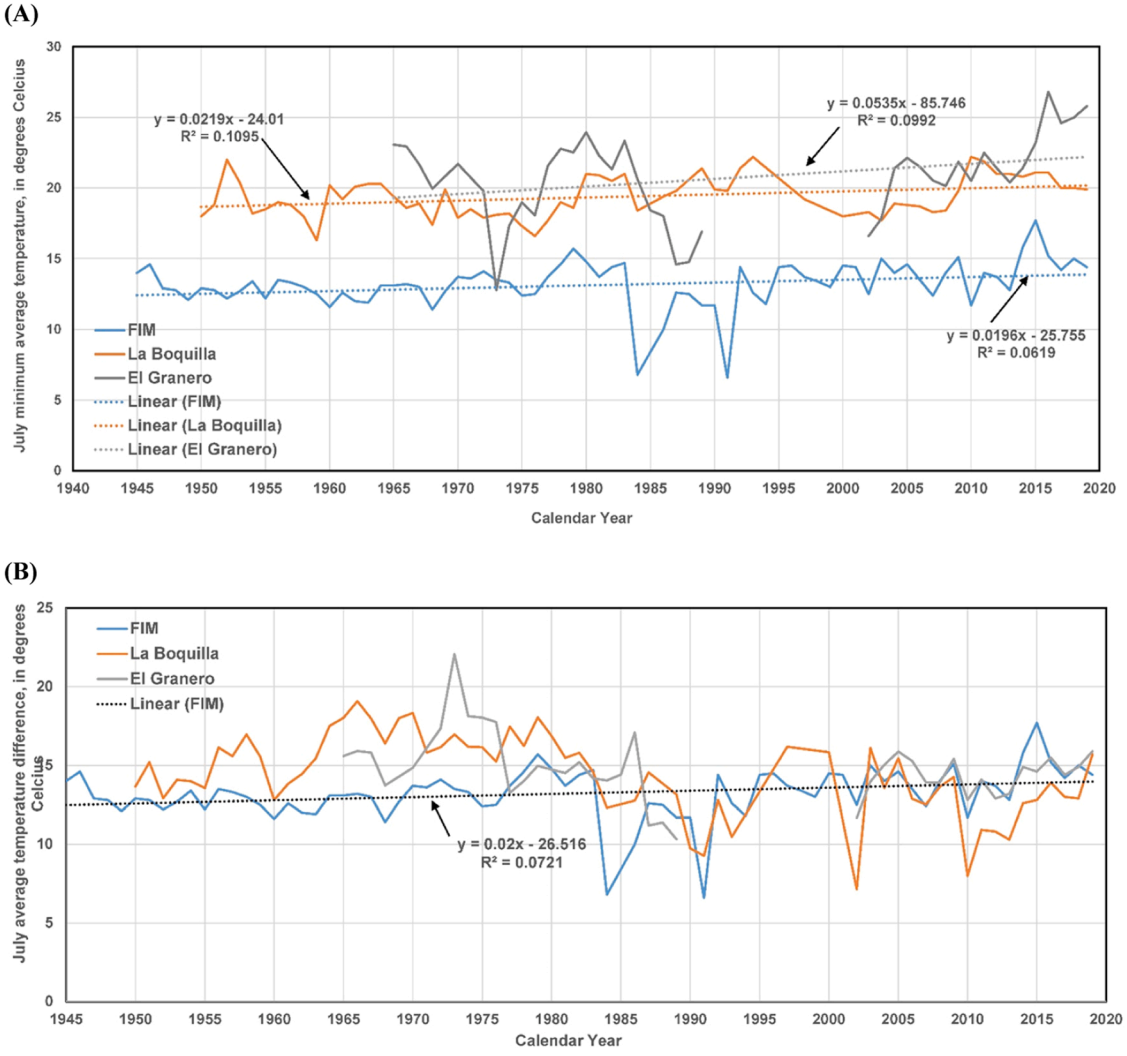

Fig. 4. Historical data of (A) Minimum July avearge temperature with linear regressions for all three reservoir sites, and (B) July temperature differences for all three reservoir locations plus linear regression for FIM reservoir temperature differences, Chihuahua, Mexico.

correlations with AMO (−0.77 at FIM; p-value <0.05); negative and positive correlations with PDO (−0.41 at La Boquilla and 0.30 at FIM; p-value <0.05); and ENSO (−0.38 at La Boquilla, 0.41 at FIM, and 0.4 at El Granero; p-value <0.05).

Long intervals of predominantly dry-years occurred during 1950–64 and 1992–2001 at La Boquilla. At FIM wet and dry-year periods were different (wet: 1968–92/2002–10, and dry:1950–67/1993–2001). The shorter record at El Granero shows more inter-annual variability with shorter wet and dry-year periods (wet: 1972–74, 1977–81, 1984–87, 1990–91, and 2003–2017, and dry: 1965–71, 1975–76, 1982–83, 1988–89, and a longer period 1992–2002).

3.1.2. Temperature

Increases in minimum temperature as well as increases and more variability of monthly average temperature differences are indicators of climate change. At FIM, the rainy-season month of July indicates the minimum temperature time series includes cycles with PDO-like periods of 37.5 and 25 years (69% of total cyclic variance) with a 7.5 year NAMS-like cycle (22%), and ENSO and ENSO-PNA-like cycles accounting for the remaining 9% of the variance (Table SM-1). The average July temperature difference shows a 25 year PDO-like cycle (91%), 8.3 year NAMS-like cycle (4.7%), and ENSO and ENSO-PNA-like cycles (2.7%) account for the rest of the variance (Table SM-1).

Average July minimum temperature and differences at FIM reservoir indicate that in the middle of the rainy season (July) there is an apparent increase in variability between the periods 1945–1984 and 1986–2019 (Fig. 4a,b). This partitioning overlaps the 1982–88 period, which is a series of El Niño and La Niña ENSO events. Over the 75-year period, the average minimum temperature at FIM increased by about 1.5 °C, which exceeds the standard deviation of the earlier period and is comparable to the more recent period. The average July temperature difference also increased by about 0.4 °C between these two historical periods. The temperature-difference standard deviation for the more recent period is 1.4 times greater than the earlier period. This suggests increased minimum temperature, temperature difference, and more variable temperature difference. This is potentially consistent with climate change and increased climate variability within climate change.

3.2. Reservoir Cycles

The cycles summarized from reservoir operations are related to analysis of supply from reservoir releases and storage, and of demand from evaporation. These reservoir-use attributes are reviewed in the context of climate variability, sustainability of surface-water supplies, and treaty delivery requirements. A detailed summary analysis of these cycles is included in the Supplementary Material.

Variability of reservoir releases is aligned with climate cycles that control runoff, but lags precipitation-based climate cycles. As with precipitation, the releases are predominantly coincident with PDO-like cycles with a lesser contribution from ENSO-like cycles (Fig. SM-2). The time series of reservoir releases shows PDO-like cycles of period ranging from 17.3 to 35 years and representing 78% (FIM) to 97% (La Boqilla) of the cyclic variability with ENSO and ENSO-PNA-like cycles providing the remainder of the variability (Table SM-1). Without additional inflows, average historical releases relative to utility capacity have total periods of delivery ranging from 3.3 years for La Boquilla, 1.5 years for FIM, and 0.4 years for El Granero, which are all less than the 5-year window of delivery obligations required under the 1944 Treaty.

Cumulative departures of releases and climate indices (fig. SM-2) show some relation to increasing PDO index and decreasing AMO index. Releases show negative correlations with AMO (−0.87 at La Boquilla, −0.49 at FIM, and −0.83 at El Granero; p-value<0.05), positive correlations with PDO (0.76 at La Boquilla and 0.57 at El Granero; p-value<0.05), and negative correlations with ENSO (−0.50 at La Boquilla; p-value<0.05). Correlation between changes in storage and climate indices, show negative correlations with AMO (−0.57 at La Boquilla and −0.90 at El Granero; p-value <0.05), positive and negative correlations with PDO (−0.48 at FIM and 0.50 at El Granero; p-value <0.05), and negative correlations with ENSO − 0.59 at FIM; p-value < 0.05). Thus storage and releases are both correlated with climate indices and appear sensitive to shorter and longer climate cycles that are longer than their utility-capacity periods of delivery.

Reservoir evaporation is a surrogate indicator for water demand and the effects of temperature on water supply. Evaporation shows positive correlations with AMO (0.90 at FIM and 0.28 at El Granero; p-value <0.05), and negative correlations with PDO (−0.28 at La Boquilla, 0.63 at FIM and −0.59 at El Granero; p-value <0.05) and with ENSO (−0.33 at La Boquilla, 0.43 at FIM and −0.65 at El Granero; p-value <0.05). Thus, evaporation as a demand on water resources shows generally opposite climate-based behavior to the supply components of storage and releases and is largest during the Spring season at all three reservoirs.

3.3. Decadal to century-scale climate cycles

Analysis of cumulative-departure of tree-ring indices that span 1278 years (733 – 2010 CE) from nearby Casas Grandes (CGCD), Chihuahua, Mexico (Figs. 2 and 5) (Cook et al., 2020) show multiple wet- and dry-periods superimposed on a much longer wet-dry cycle of about 639 years. It includes a predominantly 300-year drier period (1181–1483) followed by a protracted 477-year wetter period 1470–1947 with the mega-drought of the late 1500 s embedded in this longer wetter cycle. Cumulative departures in tree-ring and climate indices show small but significant correlations (p-value <0.05): for Casas Grandes (r = −0.2) and Tutuaca (r = −0.3) with AMO; for Casas Grandes (r = 0.4) and Tabacote-Tomochi (r = 0.5) with PDO; and minor correlations with ENSO for Casas Grandes (r = 0.2), Tabacote-Tomochi (r = 0.3), and Tutuaca (r = 0.2). The longer climate forcings of the multi-century cycles (>AMO) may be related to millennial (Zhao et al., 2021; Geel et al., 1999) and centennial (Clemens, 2005) solar cycles, and are addressed below.

Frequency analysis of the CGCD indicates longer cycles (>AMO and AMO) are present as significant contributions to decadal wet-

and dry- periods (Table SM-1). Frequency analysis indicated multiple cycles that include longer-term >AMO-like (91.8%; 107, 426, and 639 years), AMO-like (6.5%; 35–75 years), PDO-like (1.4%; 10.5–32.8 years), NAMS-like (0.2%; 7.0–10 years), ENSO-like (0.1%; 4.0–6.8 years), and ENSO-PNA-like (0.1%; 2–4 years). The cumulative departure series from tree-ring indices represent composites of these cycles, with decadal dry periods that are not always strictly coincident with the recent PDO cycles. Overall, the groups of dry years range from 12 to 43 years in duration over the past 1.2 millennia (Fig. 5). Using a 15-year window moving average based on the median cycle length of 15 years from PDO-like cyles, yielded an average number of dry years of about 8 years based on the Casas Grandes series. Thus, the 5-year delivery cycles established for the 1944 Treaty of the Rivers does not reflect the average or range of dry-year periods typical for this region over the past millennium.

Tree-ring indices from nearby Tabacote-Tomochi (Fig. 5) also indicate >AMO-like (51.5%; 137 years), AMO-like (29.8%; 58.7 years), PDO-like (16.8%; 14.7–27.4 years), NAMS-like (0.9%; 7.4–10.8 years), and ENSO plus ENSO-PNA-like (0.5%; 2–6 years) (Table SM-1). Tree-ring indices from nearby Tutuaca (Fig. 5) also indicate cycles of >AMO-like (86.4%; 120–240 years), AMO-like (7.7%; 53.2 years), PDO-like (5.2%; 11.7 and 30 years), NAMS-like (0.3%; 7.5 and 9.6 years), and0.5% of ENSO plus ENSO-PNA-like cycles.

While the series from these three sites are similar, only two show the mega-drought of the late 1500 s. The Tabacote-Tomochi trees show a different response to some of the longer-cycles such as the dry period from 1700 to 1735 as well as different amplitude that may reflect larger climate variability. Similarly, the Tutuaca index does not show the mega-drought of the late-1500 s and responds differently to the wetter periods of 1152–1568, 1829–1860, and the more recent wet period that includes the period earlier warm PDO cycle 1925–46. Like Tabacote-Tomochi, it has a different response to the recent warm PDO cycle of 1977–99. However many periods of drier conditions are common in all three series. These differences may be partly due to differences in location, higher elevation, or orographic effects that may potentially contribute to localized microclimates (Fig. 1).

3.4. Solar forcing and the millennial cycle

Time series filtered by calculation of 200-year moving average yield curves from CGCD and -Δ^{14}C that resemble each other closely (Fig. 6a), and show cyclic variation with a period of about 1000 years. Changes in ^{14}C in near-surface reservoirs lag solar luminosity changes (SLC) by about 125 years (Beer et al., 2012, Fig. 13.5.3.2–2). Two major inflection points indicate that the ^{14}C inflection points lag the CGCD inflection points by a few decades. The CGCD inflection points lag the SLC by about 90 and 75 years (Fig. 6a).

3.5. Solar forcing and century-scale cycles

The CGCD and -Δ^{14}C time series are used for correlation analysis, in the form of decadal means (Fig. 6a) in order to filter out short-period variations such as Schwabe and related cycles, each curve is detrended for analysis of millennial cycles using a third-order polynomial. Departures above and below the polynomial curves are compared for periods of 100–200 years (Fig. 6b). Some departures correspond for both CGCD and -Δ^{14}C, e.g. near 1200, 1500 and 1800 CE, but there is no consistent correspondence observed. Scatter plots of the detrended decadal means (CGCD vs. -Δ^{14}C) show no relationship except for a weak but significant correlation ($R^2 = 0.51$; p-value < 0.05) between 1700 and 1950 CE. This relation may be coincident with other factors such as the onset and growth of CO_2 emissions with increased hydrocarbon use for energy production starting with the industrial era.

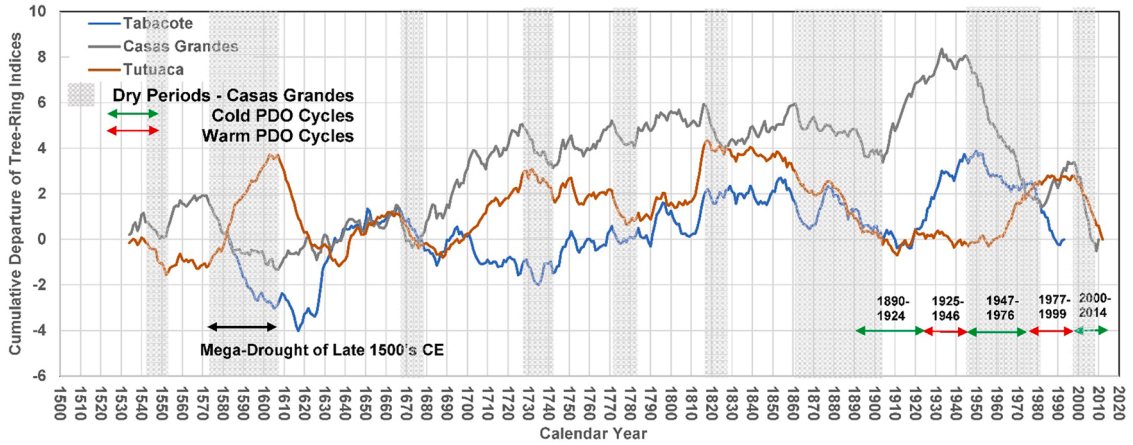

Fig. 5. Cumulative departure of tree-rings from Tabacote-Tomochi, (1583–1993) (modified from Stahle et al., 2002, 2016), Villanueva Tutuaca (1534–2012) (modified from Stahle et al., 2016) and Casas Grandes (733–2010) (modified from Cook et al., 2020) for the comparable period 1534–2010 (locations on Fig. 1) with dry-year periods estimated from the Casas Grandes tree-ring index series, and recent warm and cold PDO cycles.

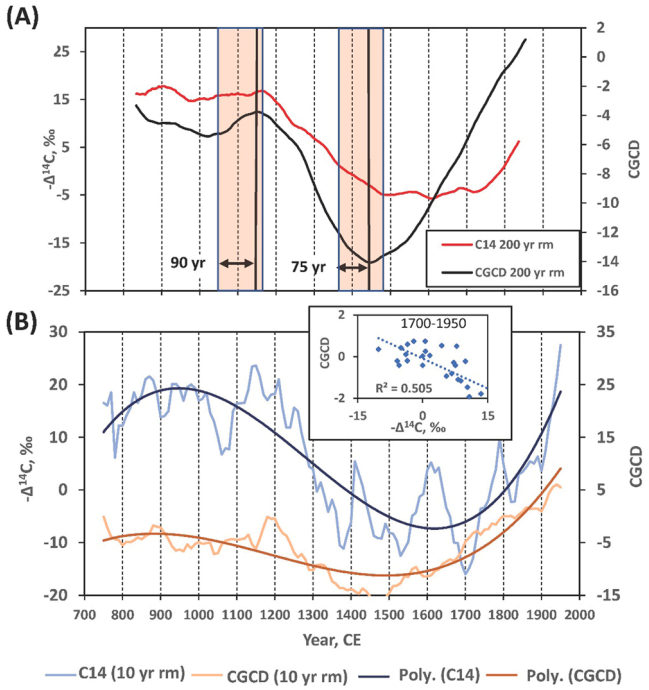

Fig. 6. Time series of (A) cumulative departures of tree-ring indices from Casas Grandes (CGCD) and -Δ^{14}C (C14) in tree rings from the western USA and Japan (from Fig. 2 of Eastoe et al., 2019). Data are presented as 200-year(A) and 10-year (B) moving averages (running mean, rm). In panel (A), the right-hand boundary of each red rectangle marks a major inflection in the -Δ^{14}C (red) curve, and the left-hand boundary marks the change in solar luminosity responsible for the inflection, given a 125-year lag. The vertical black line marks corresponding inflections of the CGCD (black) curve, and the two-headed black arrows indicate the lags between solar luminosity change and the CGCD inflections. In panel (b), third-order polynomials are fitted to the data. Departures from the C14 curve from its polynomial in general show little correspondence with departures of the CGCD curve from its polynomial. The highest degree of correlation is between decadal means of C14 and CGCD after linear de-trending (R^2 = 0.5, $p < 0.0001$) is observed between 1750 and 1950 (inset).

4. Discussion

This study has identified and evaluated the historical hydrologic cycles that have controlled recent supply from precipitation and reservoir operations and demand through temperature and evaporation. The study has also identified longer cycles that also must be

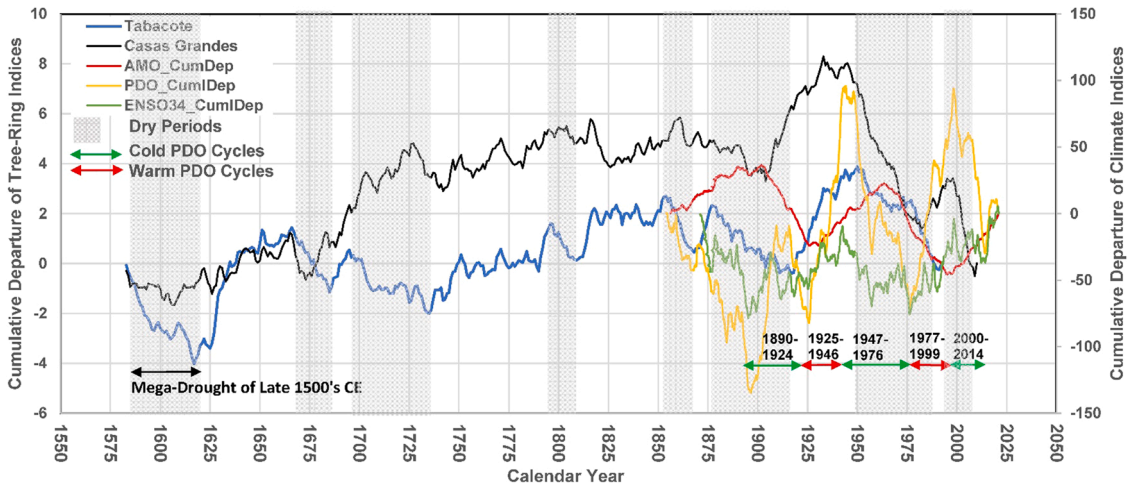

Fig. 7. Cumulative departure curves for Tabacote-Tomochi (1583–1993 CE) and Casa Grande tree-ring indices (733–2010 CE) with cumulative departure (CumDep) of the AMO, PDO and ENSO34 climate indices, dry-year periods estimated from the Tabacote-Tomochi tree-ring index series, and recent warm and cold PDO cycles.

considered for sustainability, management, and governance. This study has identified that mega-droughts and multidecadal wetter and drier periods occurr within multidecadal to multi-century cycles influenced by cycles of solar radiation from the Millenial Climate Oscillation (MCO) that need to be considered along with Anthropogenic Climate Change (ACC) to prepare for sustainability as well as treaty obligations of surface-water deliveries from the Rio Conchos watershed.

4.1. Climate Variability

Variability of precipitation in the Rio Conchos watershed is associated mainly with the phases of PDO, which modulates precipitation in winter more than in summer. The seasonality of precipitation also varies depending on the El Niño/La Niña influence, and its phase relationship with PDO and AMO cycles with positive correlation with PDO and negative correlation with AMO over different cyclic periods, as shown with tree-ring indices (Fig. 7). The shorter supply periods from precipitation are similar to the time frames of the capacity of the reservoirs. Thus, these reservoirs respond in a lagged fashion to local climate variability and related runoff. The precipitation records from these reservoir sites do not appear to show the potential effects of the 2000–2019 mega-drought (Williams et al., 2020) but instead show interaction with the composite of the climate cycles that appear to create long periods of predominantly wet-years (1965–81, 2002–04 and 2005–19); indicated as increasing cumulative departure of annual and summer precipitation (Fig. 3a). The drier-year periods observed in La Boquilla and FIM are similar to those identified in forests to southwest of Chihuahua but with oscillations of different magnitude and duration driven by climate variability (Návar and Lizárraga-Mendiola, 2013). many of these periods differ from known wet and dry-year periods from the southwestern United States, such as the severe droughts of 1976–77 and 1987–92 (Hanson, 2003), even in an area as close as Las Cruces, New Mexico that showed predominantly dry years from 2003 to 2014. This collectively may suggest that NAMS events along with ENSO events and east Pacific tropical storms may provide localized relief from the regional mega-drought identified by broader regional assessments (Williams et al., 2020; Woodhouse et al., 2012).

Modulation of winter precipitation is likely to affect long-term groundwater storage and recharge. In Chihuahua city (Fig. 1), winter precipitation for 1962–1988 made up only 22% of the annual total and had seasonal weighted mean isotope composition between winter and summer precipitation (Fig. 8) (IAEA, 2021). Groundwater isotope data for nearby Chihuahua City (Mahlknecht et al., 2008) form a broad evaporation trend of the slope near 5, originating almost entirely in winter precipitation, and probably only from large precipitation events (Fig. 8). Recharge therefore occurs mostly in winter, despite the small annual fraction of winter precipitation. Radiocarbon data from this same study also suggests that winter recharge has dominated for much of the Holocene. At least in the area near Chihuahua city, groundwater storage and recharge are likely to change in response to the PDO-related modulation of winter precipitation. Summer recharge may be present locally, as in the transboundary Upper San Pedro Basin of Arizona, where recharge in a mountain block includes 35 ± 25% summer precipitation (Wahi et al., 2008). Segregation of groundwater recharge estimates using a summer and winter ratios of mountain system recharge (Ajami et al., 2011) have been assessed for nearby transboundary Upper San Pedro Basin in Arizona, but this approach does not account for the additional climate variability from forcings such as PDO that were found to dominate in the Rio Conchos and across the Southwest (Hanson et al., 2004, 2006, Dickinson et al., 2004).

The minimum monthly temperature and temperature differences are increasing with increased climate variability. The average minimum temperature at FIM increased by about 1.5 °C over the 75-year period, which exceeds the standard deviation of the earlier period and is comparable to the more recent period (Fig. 4a). Average July temperature difference also increased by about 0.4 °C between the two historical periods (Fig. 4b), with the temperature-difference standard deviation for the more recent period 1.4 times greater than the earlier period. Global climate model estimates of Tmin indicate similar increases from the IPCC, the Sixth Assessment Report IPCC interactive atlas (IPCC, 2021) for regions coincident with the Rio Conchos Basin. Using the CMIP6 model projection, RCP-2.6, with warming 1.5°C conditions, these models allow subregional assessment of change of Tmin based on the historical period 1850-1900 for the North American Monsoon region, Northern Central America, and the Rio Grande Basin. In the Monsoon region, Tmin increased from 0.39 to 1.7°C above the average global Tmin from 1980 to 2020, with an average estimated increase of 1.6°C for the entire region. In the Northern Central America region, the Tmin increased from 0.28 to 1.5°C for the same period, average

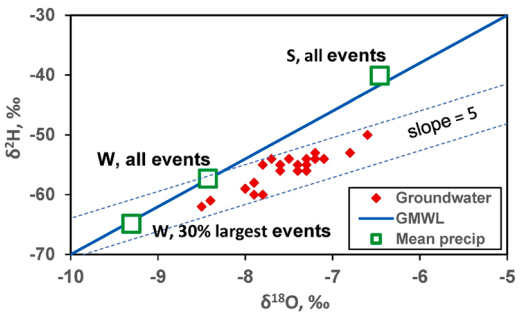

Fig. 8. Isotopic composition (δ2H vs.δ18O) for groundwater from nearby Ciudad Chihuahua area (modified from Mahlknecht et al., 2008), compared with amount-weighted seasonal means for precipitation in Ciudad Chihuahua, calculated from data for 1962–1988 (International Atomic Energy Agency, 2021). W is winter (November-May); S is summer (June-October); GMWL is the global meteoric water line, and green squares are selected mean precipitation (precip).

estimated increment of 1.2°C. Furthermore, in the Rio Grande basin region, Tmin increased from 0.19 to 1.6°C for the same period, with an average estimated increase of 1.4°C. These similar modeled and instrumental estimates of increased minimum temperature are influenced by a combination of the variable climate patterns presented here and increased concentrations of greenhouse gases in the atmoshpere.

The Mexican Drought Altas (Stahle et al., 2016) indicated that the ENSO signal has a stronger and more time-stable correlation with drought across northern Mexico than either the AMO or PDO, yet the present study clealy shows negative correlations with AMO and positive correlations with PDO and lesser correlations with ENSO indices. This is similar to the recent analysis of reconstructed streamflow from tree-ring indices also showed similar relations with AMO and PDO (Martínez-Sifuentes et al., 2020). The 70-year instrumental records analyzed here, show PDO (83 – 41%) was the largest contributors to climate variability for annual and seasonal periods for interannual to interdecadal periods and lesser conributions from ENSO (58 – 15%) (Table SM-1, fig. SM-1). Longer time intervals from tree-ring indices, show much larger and longer cycles that control multidecadal to multi-century wet and dry periods. Tree-ring indices and summer soil-moisture reconstruction (Williams et al., 2020) indicated that 2000 – 2019 mega-drought is additionally driven (by almost half, 47%) by anthropogenic climate change due to CO_2 emissions. This analysis suggests that 2000 – 2019 mega-drought may be the worst drought since the late 1500 CE mega-drought (1569–1607) across the entire sourthwest of North America, including northern Mexico. The tree-ring records from Casas Grandes and Tutuaca overlap the recent dry periods and the cold (negative) PDO cycle (1947–1976 and 2000 – 2014) (Fig. 5) and appear to be driven by the combination of these climate forcings. However, the precipitation analysis (Fig. 2) indicates wetter conditions relative to the previous protracted dry period (1992 – 2001), which is consistent with analysis from the Lower Rio Grande (Hanson et al., 2020). Together, these observations indicate that the present drought is not pervasive in this part of the US-Mexico transboundary region. In contrast, the current drought advisory (CONAGUA, 2020a, 2020b) indicates that severe drought is not developing in northern Mexico yet their analysis does not include subregional analysis or this longer context of droughts within climate variability and climate change.

In this part of northern Mexico, multidecadal droughts have occurred such as the mega-drought of the late 1500's CE (1569–1607), and more recently a protracted dry period in the 20th Century (1943–1982) that are separated by about 350 years. There are multidecadal droughts with some embedded in longer cycles of increasing wetter conditions or sustained drought. For example there is a 477 year wetter period from 1470 to 1947 that encompasses the late-1500 mega drought along with a few shorter droughts. This pattern is also similar to the GCM projections under the previous GCM A2 scenario ("business-as-usual" CO_2 emissions) analyzed for the Central Valley, California, which also showed the potential of several multidecadal droughts ocurring in the later part of the 21st Century (Hanson et al., 2012).

4.2. *Conjunctive use and sustainability*

Many transboundary conflicts focus on sharing of surface-water and do not address climate variability and conjunctive use with all water sources, including groundwater (Rivera and Hanson, 2021; Sanchez et al., 2021). Under the ISARM (International Shared Aquifer Resources Management) program (https://en.unesco.org/themes/water-security/hydrology/programmes/isarm), UNESCO and OAS recently included transboundary groundwater management (Rivera, 2015; Hanson et al., 2015) as an integral part of management of all transboundary water resources. The National Program Against Drought (Rubio Gutiérrez, 2017) was proposed as a framework for the National Drought Policy (Federman et al., 2014), developed with the Mexican Insitute of Water Technology (Cortés et al., 2016), and implemented by the National Commission of Water (CONAGUA). However, this framework shares the shortcomings of the United States NIDIS program, as it does not address conjunctive use and replenishment of water, or a more comprehensive strategy for dealing with changes in supply and demand cycles in response to long-term climate changes. This type of planning can minimize the effects of drought, support longer-term sustainability, and development of infrastructure and related governance.

Drought and sustainability of water resources are best viewed in the context of both supply-and-demand and conjunctive use. In this arid region, climate variability has driven variable supply during the period of historical record, during which the margin between supply and demand has narrowed as water consumption increases. As in many of the watersheds in the USA-MX transboundary regions about 90% of surface water and 84% of pumped groundwater are used for irrigation in the State of Chihuahua (CONAGUA, 2020b). Water-resource management must therefore be approached from an integral perspective taking longer and shorter climate cycles into account.

Conjunctive use in the Rio Conchos, is a combination of groundwater and surface-water use, that largely represents agriculture. Sustainability is driven by demand from irrigation that has grown with increased land use and changed from seasonal to permanent crops that hardened demand and intensified agricultural production that rely even more on both surface water and groundwater supply. Drought combined with agricultural intensification and hardening of demand contributed to reduced availability of surface water stored in local reservoirs. For example, drought conditions in 1994–1995, resulted in the closure of La Boquilla and FIM reservoirs to irrigation releases (Ortega-Gaucin et al., 2009). Lack of surface water was then compensated by installation of about 280 wells, which accelerated aquifer depletion and further reduced conveyance of surface water on the Rio Conchos for irrigation and treaty deliveries. Adaptation to climate varaiblility not only affects large-scale agricultur but also small-scale farmers in rural Mexico (Campos et al., 2014). Reduced supply was combined with increased demand as local farmers kept the most profitable crops. Increased irrigation demand has resulted from hardened demand from orchard crops, longer growing periods, more ET, and intensification of crop production through more density of cultivation. This evolution of supply and demand is similar to that developing in the Lower Rio Grande, where growth of irrigation demand is driven mainly by the "hardening of demand" as seasonal crops such as alfalfa and cotton are supplanted by permanent crops such as pecan orchards (Hanson et al., 2020).

The Mexican Institute of Water Technology (IMTA) estimated runoff for replenishing reservoirs in the Conchos River Basin will

decrease by 10–12% based on future scenarios of CO_2 emissions (IMTA, 2013). Therefore, agricultural lands will have less surface water for irrigation which will rely more on groundwater that will further interefere with obligated surface-water treaty deliveries, similar to ongoing water conflicts of Lower Rio Grande (Hanson et al., 2020). These projections also show wet periods, with an increase in median temperature of around 2 ℃, with a proposal to establish resource contingency plans that should be developed and implemented as soon as possible. Currently competition for water resources in the region has increased, yet there are no comprehensive water-management strategies in the region that account for the climate variability delineated in this study, resulting in conflicts over local allocation of surface water for irrigation and other uses, as well as binational treaty obligations.

Modifications to reservoir operations in Chihuahua, Mexico are controversial among farmers and local governments in Mexico. The two main demands are transboundary water deliveries and irrigation within the Rio Conchos watershed. The former are treaty obligations (USA-Mexico, 1944) and are tracked on a sliding scale of 5-year cycles, with an additional 5 years for any remaining deficits. Rio Conchos provides a large percentage of the treaty deliveries from Mexico. The 35 cycles of delivery since 1953 are generally coincident with the wet and dry-year periods from precipitation data at La Boquilla reservoir. If the total delivery for a 5-year period is achieved early within the period, then a new 5-year period begins immediately for deliveries from Mexico. Eight of the 35 cycles required the entire 5 years, and six of the eight full 5-year cycles still had a deficit delivery (10/1953 – 9/1968, 6/1982 – 6/1987, 9/1992 – 9/2007, and 10/2010 – 10/2015). Consequently, the contribution from the Rio Conchos is relatively largest during dry-year periods. The Rio Grande treaty deliveries from the USA are sustained by regional climate and snowmelt from the Southern Rocky Mountains in the Colorado headwaters of the Rio Grande. Yet deliveries for agriculture and the treaty from the Rio Conchos are dependent on local runoff from rainfall and related climate cycles (Figs. 2 and 3). To align the deliveries with the climate cycles, the delivery cycles from Mexico should be 8-15 years in length (based on the moving window analysis of Casas Grandes tree-ring data), as opposed to periods of 5 years or less (less when a reset occurs after delivery completion in less than 5 years) used by the current treaty. Overall 25 of the 35 cycles (71%) were less than 5 years and 23 cycles less than 2 years (66%). A more dynamic range of delivery periods would consider the likelihood of such short cycles, but could also take account of longer dry periods possibly with a threshold of 5 dry years. In the Casa Grandes cumulative departure tree-ring time series (Figs. 5, 6), 23% of the historical dry periods lasted 5 years or less. This threshold could potentially trigger a drought contigency for amounts and/or time periods of deliveries. The drought contingency strategy also could be similar to what is used by the USBR to reduce deliveries during drought periods for the Lower Rio Grande Project and the related 1906 Treaty (USBR, 2016, 2017, USA-Mexico, 1906).

4.3. Long-term solar forcing of climate

Both groundwater and near-surface ^{14}C are replenished by continuous small additions from the atmosphere to larger reservoirs. The sizes of the near-surface reservoirs therefore reflect long histories of replenishment at changing rates (e.g., for ^{14}C, Beer et al., 2012). Cumulative departures of tree-ring indices from long-term average values, as indicators of climate variation, might thus be more closely related than simple departures to time series such as $\Delta^{14}C$ in biomass and groundwater volumes. The similarity of the 200-year moving average curves (Fig. 6a) shows that this is the case at millennial time scale in the Rio Conchos region of northern Mexico. The similarity also indicates a strong relationship between solar luminosity and tree-ring indices, and by extension to variations in climate, at millennial time scales. Whether the climate variations involve changes in precipitation and evapotranspiration, a connection between solar luminosity and surface-water and groundwater accumulation emerges.

At century time scales, other factors, in addition to solar luminosity, are likely operating. Based on the analysis presented here, solar forcing does not appear to be consistent across the entire span of data, and where present, and accounts for half at most of observed variance. Thus additional research may be needed to better understand all of the forcings that control climate at century to millenial time periods in this region.

The lag between SLC and climate recorded in Casas Grande tree-rings constitutes a third example of lag between millennial-scale SLC and corresponding climate responses at Earth's surface. The lags reported here (about 90 and 75 years) can be compared with a 100 year lag reported by Helama et al. (2010) on the basis of tree-ring widths in Scandinavia, and 125–175 years reported by Eastoe et al. (2019) from a comparison of $\Delta^{14}C$ and $\delta^{13}C$ timeseries in sequoia tree-rings in California. Lags may differ with time and locality, but it is likely that the climatic effects of an approaching (or contemporary) millennial maximum in solar activity will not be felt until about 100 years after the solar maximum. The three studies demonstrate that the climatic response is sufficient to affect widths or $\delta^{13}C$ of tree rings.

4.4. Time Scales

This study shows cycles of drier and wetter climate at a variety of time scales. Combining tree-ring data and instrumental records indicates the importance of PDO-like cycles. Shorter cycles are indicated in the historical and recent instrumental records. These correspond to phase relationships between AMO, PDO and ENSO. Construction of reservoirs attempts to mitigate the effects of the shorter cycles and the timing disparity between supply and demand at interannual time periods. Local tree-ring data indicate cycles at 100- to 1000-year time scales, and global ^{14}C data provide evidence of solar forcing at the millennial scale.

Long climate cycles of the past, operating without human mitigation, may have contributed to the rise and fall of pre-Columbian civilizations in the region (Fig. 2). The reservoirs reflect more recent development of water-resource infrastructure to enhance reliability and sustain water-food security. Besides the mega-drought of 1569–1607 (39 years), additional dry-year periods occurred for the periods of 1666–1688 (23 years), 1695–1735 (41 years), 1798–1809 (12 years), 1853–1868 (16 years), 1875–1917 (43 years), 1952–1991 (40 years), and 1999–2012 (14 years) (Fig. 7), which are all within the range of the two modes of the PDO-like cycles. Thus

in the recent past of instrumental data and over recent centuries, the cycles are similar to the PDO-like cycles. However, the AMO and ENSO-like cycles may also be significantly contributing to the overall variation as shown in the past two centuries, as the cycles come into and out of phase with each other (Fig. 7) and collectively contribute to decadal drought periods of 12–43 years (Figs. 5 and 7).

5. Conclusions and future work

This study has provided a new data and novel assessment of climate variability in the Rio Conchos watershed over multiple time scales, and its potential effects on water supply-and-demand through analysis of climate, instrumental data, historical reservoir operations, changes in ^{14}C concentrations, and tree-ring indices. Multiple levels of climate variability occur from interannual and interdecadal to multi-century and millenial periods. Unlike some previous studies of this region, at multi-decade scales, estimated climate cycles are predominantly PDO-like cycles, with additional but lesser contributions by AMO and ENSO-like cycles. Mega-droughts and periodic multidecadal droughts occur within climate cycles at 100- to 1000-year time scales. Climate variability including MCO, now combined with climate change (ACC), will dictate future cycles of supply and demand that will require mitigation and management to achieve sustainability and reliability. In turn, sustainability will require conjunctive use to not only reduce the effects of demand but also to enhance the effects of supply and related replenishment during periodic wet periods.

The 5-year cycle of transboundary water deliveries under the 1944 Treaty of the Rivers is inadequate for management of the Rio Conchos watershed, where droughts average about 8 years within the median 15-year window of PDO-like cycles, and longer dry periods span 12–43 years. The delivery agreement of the Treaty may also benefit from an additional drought contingency and some kind of threshold metric that initiates a drought contingency for protracted or severe droughts. Reservoir operation strategies reflecting the longer climate cycles may serve local and national communities better than strategies at present required by the 1944 Treaty. Improved strategies are required as competition for water increases because of changes in land use and shifts to more profitable perennial crops.

This study has identified frequencies and correlations of climate variability over a broad spectrum of time periods. While correlation does not constitute causation, these analysis provide a basis for understanding the context of climate variability by using a wide variety of data types and time periods, and provides higher-order observations that can help develop integrated modeling of the processes that control the use and movement of water resources. Future holisitc analysis of adaptation and mitigation strategies taking account of climate variability will require an integrated hydrologic model (Boyce et al., 2020) that can simulate and assess the conjunctive use and movement of water at the multiple time scales of climate cycles identified in this work. This could be similar to the analysis and modeling of the Lower Rio Grande Operating Agreement by USBR (USBR, 2008) performed to evaluate deliveries under historical Climate variability (Hanson et al., 2020) and potential future climate change (USBR, 2016, 2017; Ferguson and Llewellyn, 2015). While some analysis has been performed locally (DOF, 2011), future work will need to develop an integrated hydrologic model that can replicate these climate cycles, use and movement of water and related changes in land use, and simulate the related physical processes of supply and demand. This will provide a neutral and comprehensive avenue of analysis and management and assess the proportions and timing of supply and demand components that includes reservoir operations. This, in turn, will provide a vehicle for combined analysis of sustainable allocation of surface water and groundwater across the watershed as well as possible framework for adjustments in management and governance of all water resources and related land use.

CRediT authorship contribution statement

Marusia Renteria-Villalobos: Conceptualization, Methodology, Software, Formal analysis, Visualization, Investigation, Writing – original draft. **Randall Hanson**: Conceptualization, Methodology, Software, Formal analysis, Supervision, Visualization, Investigation, Validation, Writing – original draft, Writing – review & editing. **Christopher Eastoe:** Conceptualization, Methodology, Software, Formal analysis, Supervision, Visualization, Investigation, Validation, Writing – review & editing.

Declaration of Competing Interest

The authors declare that they have no known competing financial interests or personal relationships that could have appeared to influence the work reported in this paper.

Acknowledgements

The authors would like to thank the Mexican governmental institutions: CONAGUA (Comisión Nacional del Agua), JCAS-Chihuahua (Junta Central de Agua y Saneamiento, Chihuahua), and SIAP (Servicio de Información Agroalimentaria y Pesquera), for providing the historical data for reservoirs, climate, and crop-production. We are also grateful with Dr. Edward Cook (Lamont-Doherty Earth Observatory) for his technical support and thank him for providing the exceptional tree-ring index record for Casas Grandes, Mexico.

Appendix A. Supporting information

Supplementary data associated with this article can be found in the online version at doi:10.1016/j.ejrh.2022.101207.

References

Adams, D.K., Comrie, A.C., 1997. The North American monsoon. Bull. Am. Meteorol. Soc. 78 (10), 2197–2213.

Ajami, H., Meixner, T., Dominguez, F., Hogan, J., Maddock III, T., 2011. Seasonalizing mountain system recharge in semi-arid basins-climate change impacts. Groundwater 13. https://doi.org/10.1111/j.1745-6584.2011.00881.x.

Alley, R.B., 2003. Paleoclimatic insights into future climate challenges. Philos. Trans. R. Soc. Lond. 361, 1831–1849.

Anderegg, L.D.L., Anderegg, W.R.L., Berry, J.A., 2013. Not all droughts are created equal: translating meteorological drought into woody plant mortality. Tree Physiol. 33, 701–712. https://doi.org/10.1093/treephys/tpt044.

Asmerom, Y., Polyak, V.J., Rasmussen, J.B.T., Burns, S.J., Lachniet, M., 2013. Multidecadal to multicentury scale collapses of Northern Hemisphere monsoons over the past millennium (http://www.pnas.org/cgi/doi/). PNAS 110 (24), 9651–9656. https://doi.org/10.1073/pnas.1214870110/.

Beer, J., McCracken, K., von Steiger, R., 2012. Cosmogenic Radionuclides: Theory and Applications in the Terrestrial and Space Environments. Springer, Berlin, Germany. https://doi.org/10.1007/978-3-642-14651-0.

Boyce, S.E., Hanson, R.T., Ferguson, I., Schmid, W., Henson, W., Reimann, T., Mehl, S.M., Earll, M.M., 2020. One-water hydrologic flow model: a MODFLOW based conjunctive-use simulation software. U. S. Geol. Surv. Tech. Methods 6–A60, 435.

Braun, H., 2005. Possible solar origin of the 1,470-year glacial climate cycle demonstrated in a coupled model. Nature 438, 208–211.

Campos, M., Velázquez, A., McCall, M., 2014. Adaptation strategies to climatic variability: a case study of small-scale farmers in rural Mexico. Land Use Policy 38, 533–540.

Cayan, D.R., Dettinger, M.D., Diaz, H.F., Graham, N.E., 1998. Decadal variability of precipitation over western North America. J. Clim. 11, 3148–3166.

Cervera Gómez, L.E., 2008. Impacts of droughts on the Rio Conchos watershed over the international water treaty between Mexico and the United States of America. Nóesis. Rev. De. Cienc. Soc. Y. Humanid. 17 (33), 116–118.

Clemens, S.C., 2005. Millennial-band climate spectrum resolved and linked to centennial-scale solar cycles. Quat. Sci. Rev. 24 (5–6), 521–531. https://doi.org/10.1016/j.quascirev.2005.10.015.

Compo, G.P., Whitaker, J.S., Sardeshmukh, P.D., Matsui, N., Allan, R.J., Yin, X., Gleason, B.E., Vose, R.S., Rutledge, G., Bessemoulin, P., Brönnimann, S., Brunet, M., Crouthamel, R.I., Grant, A.N., Groisman, P.Y., Jones, P.D., Kruk, M., Kruger, A.C., Marshall, G.J., Maugeri, M., Mok, H.Y., Nordli, Ø., Ross, T.F., Trigo, R.M., Wang, X.L., Woodruff, S.D., Worley, S.J., 2011. The twentieth century reanalysis project. Q. J. Roy. Meteorol. Soc. 137, 1–28. https://doi.org/10.1002/qj.776.

CONAGUA, 2020a. Monitor de sequía en México. ⟨https://smn.conagua.gob.mx/es/climatologia/monitor-de-sequia/monitor-de-sequia-en-mexico/⟩.

CONAGUA. 2020b. Registro público de derechos de agua (REPDA). ⟨http://sina.conagua.gob.mx/sina/tema.php?tema=usosAgua&ver=reporte&o=0&n=nacional⟩.

Cook, E.R., Woodhouse, C.A., Eakin, C.M., Meko, D.M., Stahle, D.W., 2004. Long-term aridity changes in the Western United States. Science 306 (5698), 1015–1018. https://doi.org/10.1126/science.1102586.

Cook, E.R., Jacoby, G.C., D'Arrigo, R., Buckley, B.M., Anchukaitis, K. and Pederson, N., 2020. Tree-ring research. ⟨https://www.ldeo.columbia.edu/research/biology-paleo-environment/tree-ring-research-laboratory⟩.

Cortés, F.A., Pérez, M.L., Federman, D.K., Ortega-Gaucin, D., 2016. The national drought policy in Mexico. J. Energy Chall. Mech. 3 (3), 157–166.

Deser, C., Alexander, M.A., Xie, S.-P., Phillips, A.S., 2010. Sea surface temperature variability: patterns and mechanisms. Annu. Rev. Mar. Sci. 2010 2, 115–143, 31.

Dettinger, M.D., Ghil, M., Strong, C.M., Weibel, W., You, P., 1995. Software expedites singular-spectrum analysis of noisy time series. EOS, Trans. Am. Geophy Union 76 (2), 12–21.

Dickinson, J.E., Hanson, R.T., Ferré, T.P.A., Leake, S.A., 2004. Inferring time-varying recharge from inverse analysis of long-term water levels. Water Res. Res. 40 (7), 15.

Dickinson, J.E., Hanson, R.T., Predmore, S.K., 2014. HydroClimATe—hydrologic and climatic analysis toolkit. U. S. Geol. Surv. Tech. Methods 4–A9, 49. https://doi.org/10.3133/tm4a9.

DOF (Diario Oficial de la Federación), 2011. Acuerdo por el que se da a conocer el resultado de los estudios técnicos de la Región Hidrológica número 24 Bravo-Conchos. S. d. Gobernación. México, Secreataría de Gobernación.

Eastoe, C.J., Dettman, D.L., 2016. Isotope amount effects in hydrologic and climate reconstructions of monsoon climates: implications of some long-term data sets for precipitation. Chem. Geol. 460, 76–89.

Eastoe, C.J., Tucek, C.S., Touchan, R., 2019. $\delta^{14}C$ and $\delta^{13}C$ in annual tree-ring samples from Sequoiadendron giganteum, AD 998-1510: solar cycles and climate. Radiocarbon 61 (3), 661–680. https://doi.org/10.1017/RDC.2019.27.

Ehsani, N., Vörösmarty, C.J., Fekete, B.M., Stakhiv, E.Z., 2017. Reservoir operations under climate change: storage capacity options to mitigate risk. J. Hydr. 555, 435–446.

ENC, 2021. Millennial Climate Oscillations. ⟨https://www.encyclopedia.com/environment/energy-government-and-defense-magazines/millennial-climate-oscillations⟩.

Enciso, A., 2020. Conagua modificará estrategia para enviar agua a EU. La Jornada. México. La Jorn. 3.

Erb, M.P., Emile-Geay, J., Hakim, G.J., Steiger, N., Steig, E.J., 2020. Atmospheric dynamics drive most interannual U.S. droughts over the last millennium. Sci. Adv6 12.

Fagan, B., 2008. The Great Warming: Climate Change and the Rise and Fall of Civilizations. Bloomsbury Press, New York, p. 282.

Faunt, C.C. (Eds.), Hanson, R.T., and Belitz, K., 2009. Ground-water availability of the Central Valley aquifer, California. U.S. Geological Survey Professional Paper 1766, 212, https://doi.org/10.3133/pp1766.

Federman, D.K., Cortés, F.A., Pérez, M.L., 2014. Constructing a framework for National Drought Policy: the way forward in Mexico. Weather Clim. Extrem. 3, 90–94.

Ferguson, I.A., Llewellyn, D., 2015. Simulation of Rio grande project operations in the rincon and mesilla basins: summary of model configuration and results. U. S. Bur. Reclam. Tech. Memo. 56. No. 86-68210–2015-05.

Geel, B. van, Raspopov, O.M., Renssen, H., Plicht, Jvan der, Dergachev, V.A., Meijerd, H.A.J., 1999. The role of solar forcing upon climate change. Quat. Sci. Rev. 18 (3), 331–338. https://doi.org/10.1016/S0277-3791(98)00088-2.

Gurdak, J.J., Hanson, R.T., Green, T.R., 2009. Effects of climate variability and change on groundwater resources of the United States. U. S. Geol. Surv. Fact. Sheet FS09–3074, 4.

Gutierrez, M., Johnson, W., Mickus, K., 2004. Watershed assessment along a segment of the Rio Conchos in Northern Mexico using satellite images. J. Arid Environ. 56, 395–412.

Gutzler, D.S., 2004. An index of interannual precipitation variability in the core of the North American Monsoon region. J. Clim. 17, 4473–4480.

Hanson, R.T., 2003. Geohydrologic framework of recharge and seawater intrusion in the Pajaro Valley, Santa Cruz and Monterey Counties, California. U. S. Geol. Surv. Water-Resour. Investig. Rep. WRIR03 4096, 88.

Hanson, R.T., 2015. Hydrologic framework of the Santa Clara Valley, California. GSA Geosph. 11 (3), 606–637.

Hanson, R.T., Martin, P., Koczot, K.M., 2003. Simulation of ground-water/surface-water flow in the Santa Clara-Calleguas Basin. Calif. U. S. Geol. Surv. Water-Resour. Investig. Rep. 02–4136, 214.

Hanson, R.T., Newhouse, M.W., Dettinger, M.D., 2004. A methodology to assess relations between climatic variability and variations in hydrologic time series in the southwestern United States. J. Hydrol. 287 (1), 252–269.

Hanson, R.T., Dettinger, M.D., Newhouse, M.W., 2006. Relations between climatic variability and hydrologic time series from four alluvial basins across the southwestern United States. Hydrogeol. J. l 14 (7), 1122–1146.

Hanson, R.T., Izbicki, J.A., Reichard, E.G., Edwards, B.D., Land, M., Martin, P., Lee, H.J., Normark, W.R., 2009. Comparison of groundwater flow. In: Southern California coastal aquifers. Earth Science in the Urban Ocean, 454. The Southern California Continental Borderland, GSA, pp. 345–373.

Hanson, R.T., Flint, L.E., Flint, A.L., Dettinger, M.D., Faunt, C.C., Cayan, D., Schmid, W., 2012. A method for physically based model analysis of conjunctive use in response to potential climate changes. Water Res. Res. 48 (6), 23.

Hanson, R.T., Rivera, A., Tujchneider, O., Guillén, C., Campos, M., Da Franca, N., May, Z., and Aureli, A., 2015. A regional strategy for the assessment and management of transboundary aquifer systems in the Americas. 2015: AGU H51A-1350.
Hanson, R.T., Ritchie, A.B., Boyce, S.E., Galanter, A.E., Ferguson, I.A., Flint, L.E., Flint, A.L., Henson, W.R., 2020. Rio Grande transboundary integrated hydrologic model and water-availability analysis, New Mexico and Texas, United States, and northern Chihuahua, Mexico. U. S. Geol. Surv. Sci. Investig. Rep. 2019–5120, 186.
Hegerl, G.C., Zwiers, F.W., Braconnot, P., Gillett, N.P., Luo, Y., Marengo Orsini, J.A., Nicholls, N., Penner, J.E., Stott, P.A., 2007. Understanding and attributing climate change. In: Solomon, S., Qin, D., Manning, M., Chen, Z., Marquis, M., Averyt, K.B., Tignor, M., Miller, H.L. (Eds.), Climate Change 2007: The hysical Science Basis. contribution of working group I to the Fourth Assessment Report of the Intergovernmental Panel on Climate Change, 84. Cambridge University Press, Cambridge, United Kingdom and New York. ⟨https://www.ipcc.ch/site/assets/uploads/2018/02/ar4-wg1-chapter9-1.pdf/⟩.
Helama S., Fauria M., Mielikainen K., Timonen M., Eronen M. 2010. Sub-Milankovitch solar forcing of past climates: mid and late Holocene perspectives. Geol Soc of Amer Bull 122(11/12):1981–1988.
Henley, B.J., Gergis, J., Karoly, D.J., Power, S.B., Kennedy, J., Folland, C.K., 2015. A tripole index for the interdecadal Pacific oscillation. Clim. Dyn. 45 (11–12), 3077–3090. https://doi.org/10.1007/s00382-015-2525-1. ⟨https://psl.noaa.gov/data/timeseries/IPOTPI/⟩.
Hu, Q.S., Feng, S., 2012. AMO- and ENSO-driven summertime circulation and precipitation variations in North America: papers in natural resources. 387. Univ. Neb. Linc. 6477–6495.
IBWC/CILA, 2020, Act 325: Measures to conclude the current cycle of water deliveries from the Rio Bravo without failure, to provide humanitarian support for the municipal supply of water for the Mexican populations, and to establish mechanisms of future cooperation, and better predictability and confidence of strategies of water from the Rio Bravo to users in Mexico and the United States, 5. ⟨https://www.ibwc.gov/Treaties_Minutes/Minutes.html/⟩.
IMTA, 2013. Desarrollo de un portafolio priorizado de medidas de adaptación públicas identificadas para el sector agrícola. Inf. Final PROYECTO RD-1238. México 389.
INEGI, 2017. Anuario estadístico y geográfico de Chihuahua. Inst. Nac. De. Estad. Y. Geogr. ⟨https://www.inegi.org.mx/app/biblioteca/ficha.html?upc=702825092139⟩.
International Atomic Energy Agency (IAEA), 2021. Global network of isotopes in precipitation, WISER Database. http//www-naweb.iaea.org/napc/ih/IHS_resources_gnip.html/.
IPCC, 2021. IPCC WGI Interactive Atlas - Regional Information: https://interactive-atlas.ipcc.ch/.
JCAS, 2013. Evaluación de las fuentes actuales de abastecimiento a la ciudad de Chihuahua, estudio de factibilidad de fuentes alternas y anteproyecto de infraestructura hidráulica necesaria, Acuífero: Chihuahua-Sacramento. Mex., Junta Cent. De. Agua Y. Saneam. 136.
Kuss, A.J.M., Gurdak, J.J., 2014. Groundwater level response in U.S. principal aquifers to ENSO, NAO. PDO, Amo. J. Hyd 519, 1939–1952.
Mahlknecht, J., Horst, A., Hernández-Limón, G., Aravena, R., 2008. Groundwater geochemistry of the Chihuahua City region in the Rio Conchos Basin, (northern Mexico) and implications for water resource management. Hyd Proc. 22 (24), 4736–4751.
Malamud-Roam, F.P., Ingram, B.L., Hughes, M., Florsheim, J.L., 2006. Holocene paleoclimate records from a large California estuarine system and its watershed region: linking watershed climate and bay conditions. Quat. Sci. Rev. 25 (13), 1570–1598.
Mann, M.E., Zhang, Z., Rutherford, S., Bradley, R.S., Hughes, M.K., Shindell, D., Ammann, C., Faluvegi, G., Ni, F., 2009. Global signatures and dynamical origins of the Little Ice Age and Medieval Climate Anomaly. Science 326, 1256–1260. https://doi.org/10.1126/science.1177303.
Mantua, N.J., Hare, S.R., 2002. The Pacific Decadal Oscillation. J. Oceonagr 58, 35–44. https://doi.org/10.1023/A:10158 20616 384.
Mantua, N.J., Hare, S.R., Zhang, Y., Wallace, J.M., Francis, R.C., 1997. A Pacific interdecadal climate oscillation with impacts on salmon production. Bull. Am. Meteor. Soc. 78, 1069–1079.
Martínez-Sifuentes, A.R., Villanueva-Díaz, J., Carlón-Allende, T., Estrada-Ávalos, J., 2020. 243 years of reconstructed streamflow volume and identification of extreme hydroclimatic events in the Conchos River Basin, Chihuahua, Mexico. Springe Nat.: Trees 15. https://doi.org/10.1007/s00468-020-02002-w.
McCabe, G.J., Dettinger, M.D., 1999. Decadal variations in the strength of ENSO teleconnections with precipitation in the western United States. Int. J. Climatol. 19, 1399–1410.
McCabe, G.J., Palecki, M.A., Betancourt, J.L., 2004. Pacific and Atlantic Ocean influences on multidecadal drought frequency in the United States. PNAS, Natl. Acad. Sci. 101 (12), 4136–4141.
Meehl, G.A., Hu, A., 2006. Megadroughts in the Indian monsoon region and southwest North America and a mechanism for associated multidecadal Pacific sea-surface temperature anomalies. J. Clim. 19, 1605–1623.
Milly, P.C.D., Betancourt, J., Falkenmark, M., Hirsch, R.M., Kundzewicz, Z.W., Lettenmaier, D.P., Stouffer, R.J., 2008. Stationarity is dead: whither water management? Science 319 (5863), 573–574.
Milly, P.C.D., Betancourt, J., Falkenmark, M., Hirsch, R.M., Kundzewicz, Z.W., Lettenmaier, D.P., Stouffer, R.J., Dettinger, M.D., Krysanova, V., 2015. On critiques of "Stationarity is dead: whither water management?". Water Res. Res. 51 (9), 7785–7789.
Miyahara, H., Masuda, K., Furuzawa, H., Menjo, H., Muraki, Y., Kitagawa, H., Nakamura, T., 2004. Variation of the radiocarbon content in tree rings during the Spoerer minimum. Radiocarbon 46 (2), 965–968.
Miyake, F., Nagaya, K., Masuda, K., Nakamura, T., 2012. A signature of cosmic-ray increase in AD 774–775 from tree rings in Japan. Nature 486 (7402), 240–242. https://doi.org/10.1038/nature11123.
Miyake, F., Masuda, K., Nakamura, T., 2013. Lengths of Schwabe cycles in the seventh and eighth centuries indicated by precise measurement of carbon-14 content in tree rings. J. Geophy Res: Space Phys. 118 (12), 7483–7487. https://doi.org/10.1002/2012JA018320.
Mu, J.E., Ziolkowska, J.R., 2018. An integrated approach to project environmental sustainability under future climate variability: An application to U.S. Rio Grande Basin. Ecol. Indic. 95, 654–662. https://doi.org/10.1016/j.ecolind.2018.07.066/.
Mumme, S., 2019. The 1944 U.S.-Mexico Water Treaty as a constitutional document. Mexico Center, USA. Rice University's Bak. Inst. Public Policy 14.
Návar, J., Lizárraga-Mendiola, L., 2013. Hydro-climatic variability and forest fires in Mexico's northern temperate forests. Geofísica Int. 52 (1), 5–20.
Newman, M., Compo, G.P., Alexander, M.A., 2003. ENSO-forced variability of the Pacific decadal oscillation. J. Clim. 16, 3853–3857.
Newman, M., Alexander, M.A., Ault, T.R., Cobb, K.M., Deser, C., Di Lorenzo, E., Mantua, N.J., Miller, A.J., Minobe, S., Nakamura, H., Schneider, N., Vimont, D.J., Phillips, A.S., Scott, J.D., Smith, C.A., 2016. The Pacific decadal oscillation, revisited. J. Clim. 4399–4427. https://doi.org/10.1175/JCLI-D-15-0508.1.
Nigam, S., Guan, B., Ruiz-Barradas, A., 2011. Key role of the Atlantic Multidecadal Oscillation in 20th century drought and wet periods over the Great Plains. Geophys. Res. Let. 38 (L16713), 6. https://doi.org/10.1029/2011GL048650.
NOAA_AMO, 2020. NOAA Physical Sciences Laboratory, AMO unsmoothed, ⟨http://www.psl.noaa.gov/data/timeseries/AMO/⟩, Accessed February 2, 2021.
NOAA_ENSO, 2020. NOAA NINA34 HadISST (^{5}N–^{5}S 170W-120W), ⟨https://psl.noaa.gov/gcos_wgsp/Timeseries/Nino34/⟩, Accessed February 2, 2021.
NOAA_PDO, 2020. NOAA National Centers for Environmental Information, ⟨https://www.ncdc.noaa.gov/teleconnections/pdo/⟩, Accessed February 2, 2021.
Parsons, L.A., Coats, S., Overpeck, J.T., 2018. The continuum of drought in southwestern North America. J. Clim. 31, 8627–8643. https://doi.org/10.1175/JCLI-D-18-0010.1.
Rivera, A. (Eds), 2015. Estrategia regional para la gestión de los sistemas de acuíferos transfronterizos (SAT) en las Americas (regional strategy for the management of transboundary aquifers systems in the Americas). Paris, France, UNESCO/OEA–ISARM AMERICAS Book IV, 205.
Rivera, A., and Hanson R.T., 2021. State of affairs of models and governance of transboundary aquifers along the Mexico-U.S. border. ISARM2021, 2nd International Conference Transboundary Aquifers Challenges and the way forward, December 6–9, 2021, UNESCO, Paris, France, https://isarm2021.org/.
Rubio Gutiérrez, H., 2017. National Program Against Drought (PRONACOSE). Predict, Plan, Prepare: How to Stop Drought Becoming Famine Seminar. FAO, Italy.
Saldaña, T.M., 2012. Water rituals on the Bravo/Grande River: a transnational political and ecological inheritance. J. Political Ecol. 19 (1), 57–69.
Salzer, M.W., Kipfmueller, K.F., 2005. Reconstructed temperature and precipitation on a millennial timescale from Tree-Rings in the southern Colorado Plateau, U.S. A. Clim. Change 70 (3), 465–487.

Sanchez, R., Breña-Naranjo, J.A., Rivera, A., Hanson, R.T., Hernández-Espriú, A., Hogeboom, R.J., Milman, A., Benavides, J.A., Pedrozo-Acuña, A., Soriano-Monzalvo, J.C., Megdal, S.B., Eckstein, G., Rodriguez, L., 2021. Binational reflections on pathways to groundwater security in the Mexico–United States borderlands. Water Int. 26 (7–8), 1017–1036. https://doi.org/10.1080/02508060.2021.1999594.

Seager, R., Ting, M., 2017. Decadal drought variability over North America. Mechanisms and predictability. Curr. Clim. Change Rep. 3, 141–149.

SIAP (Servicio de Información Agroalimentaria y Pesquera), 2020. Cierre de producción agrícola Mexico.

SINA-CONAGUA, 2018. Distritos y unidades de riego, Subdirección General de Infraestructura Hidroagrícola, ⟨http://sina.conagua.gob.mx/sina/tema.php?tema=distritosriego/⟩.

Stahle, D.W.; Burns, B.T.; Cleaveland, M.K., 2002 (2002–05-21): NOAA/WDS Paleoclimatology - Stahle - El Tabacote and Tomochic - PSME - ITRDB MEXI028. NOAA National Centers for Environmental Information. ⟨https://doi.org/10.25921/pnj6–8n88⟩, Accessed April 27, 2020.

Stahle, D.W., Cook, E.R., Burnette, D.J., Villanueva, J., Cerano, J., Burns, J.N., Griffin, D., Cook, B.I., Acuña, R., Torbenson, M.C.A., Szejner, P., Howard, I.M., 2016. The Mexican Drought Atlas: Tree-ring reconstructions of the soil moisture balance during the late pre-Hispanic, colonial, and modern eras. Quat. Sci. Rev. 149, 34–60.

Stuiver, M., Reimer, P.J., Braziunas, T.F., 1998. High-precision radiocarbon age calibration for terrestrial and marine samples. Radiocarbon 40 (3), 1127–1151.

USA-Mexico, 1906. Convention between the United States and Mexico, equitable distribution of the waters of the Rio Grande: Signed at Washington, May 21, 1906; Ratification advised by the Senate June 26, 1906; Ratified by the President December 26, 1906; Ratified by Mexico January 5, 1907; Ratifications exchanged at Washington January 16, 1907; Proclaimed January 16, 1907, by the President of the United States, Theodore Roosevelt: Washington, D.C., United States of America, 3.

USA-Mexico, 1944. 1944 treaty concerning the utilization of waters of the Colorado and Tijuana Rivers and of the Rio Grande. Wash., D. C., USA, USA Repub. Mex. 1944, 12.

USBR, 2008. Operating Agreement for the Rio Grande Project. 23, URL ⟨http://www.usbr.gov/uc/albuq/rm/RGP/pdfs/Operating-Agreement2008.pdf/⟩.

USBR, 2016. Continued implementation of the 2008 operating agreement for the Rio Grande Project. N. Mex. Tex. Environ. Impact Statement.: U. S. Bur. Reclam. 582.

USBR, 2017. Rio Grande operating agreement environmental impact statement. U. S. Bur. Reclam. 4.

Velasco, E.M., Gurdak, J.J., Dickinson, J.E., Ferré, T.P.A., Corona, C.R., 2017. Interannual to multidecadal climate forcings on groundwater resources of the U.S. West Coast. J. Hyd: Reg. Stud. 11, 250–265.

Vörösmarty, C.J., Green, P., Salisbury, J., Lammers, R.B., 2000. Global water resources: vulnerability from climate change and population growth. Science 289 (5477), 284–288.

Wahi, A.K., Hogan, J.F., Ekwurzel, B., Baillie, M.N., Eastoe, C.J., 2008. Geochemical quantification of semiarid mountain recharge. Ground Water 46, 414–425.

Walsh, C., 2009. To come of age in a dry place: Infrastructures of irrigated agriculture in the Mexico-U.S. Borderlands. Southern. Rural Sociol. 24 (1), 21–43.

Williams, A.P., Cook, E.R., Smerdon, J.E., Cook, B.I., Abatzoglou, J.T., Bolles, K., Baek, S.H., Badger, A.M., Livneh, B., 2020. Large contribution from anthropogenic warming to an emerging North American megadrought. Science 368 (6488), 314–318.

Woodhouse, C.A., Lukas, J.J., 2006. Multi-century tree-ring reconstructions of Colorado streamflow for water resource planning. Clim. Change 78 (2), 293–315.

Woodhouse, C.A., Stahle, D.W., Díaz, J.V., 2012. Rio Grande and Rio Conchos water supply variability over the past 500 years. Clim. Res 51, 125–136. https://doi.org/10.3354/cr01059.

Young-Min, Y., Soon-Il, A., Bin, W., Park, J.H., 2020. A global-scale multidecadal variability driven by Atlantic multidecadal oscillation. Natl. Sci. Rev. 7, 1190–1197. https://doi.org/10.1093/nsr/nwz216.

Zhao, X., Soon, W., Velasco Herrera, V.M., 2021. Holocene millennial-scale solar variability and the climatic responses on Earth. Universe 7 (36), 11. https://doi.org/10.3390/universe7020036.